Climate Modeling for Global Warming Projection at the MRI

Akira Noda and MRI-CGCM modeling group
Meteorological Research Institute

- Transient runs with MRI-CGCMs
- Downscaling with MRI regional climate models
- Earth system modeling for the carbon cycle and chemical mass transport

Climate Modeling at MRI

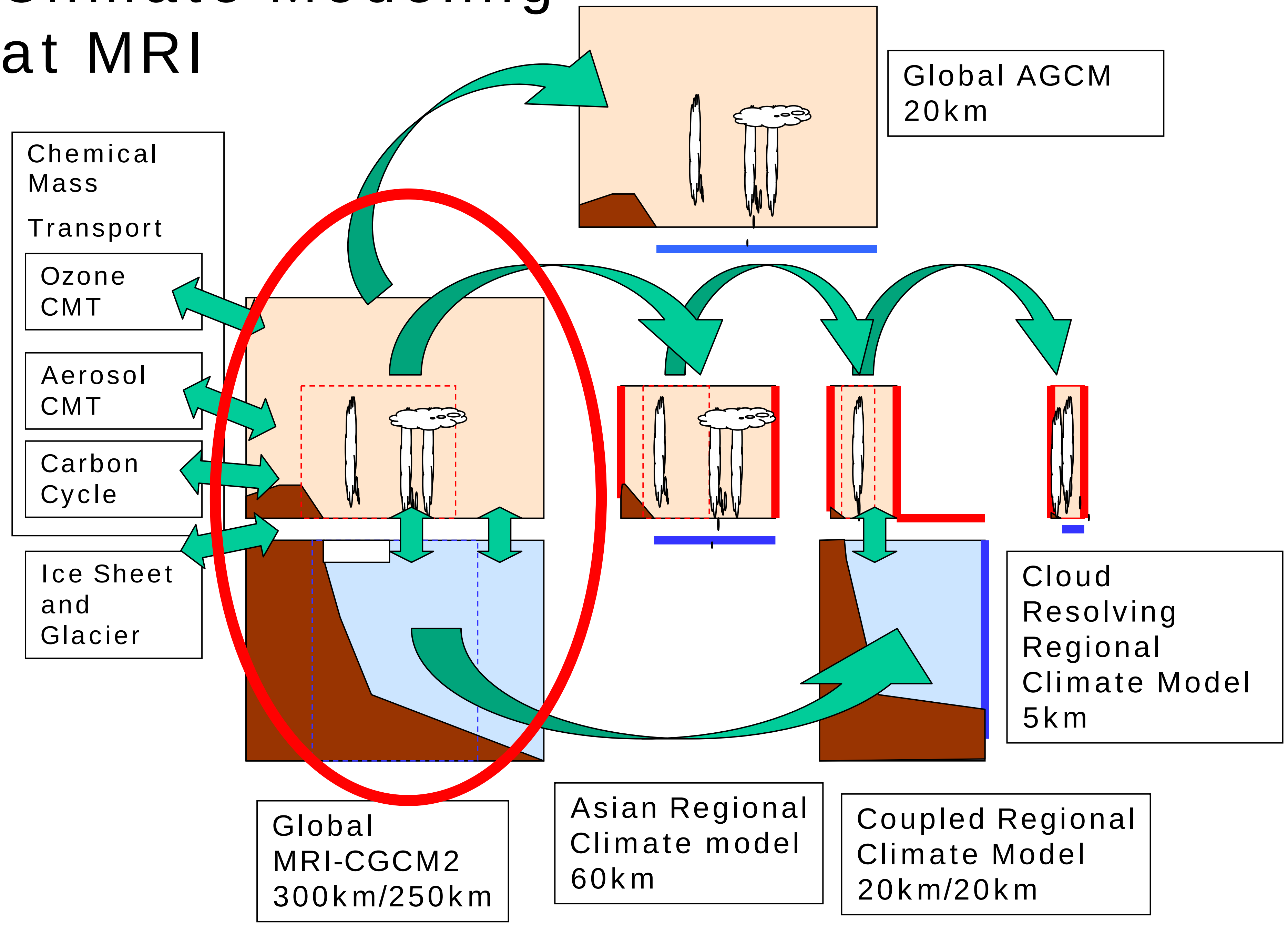

Feature	MRI-CGCM1	MRI-CGCM2
	Atmospheric component	
Horizontal resolution	5° (long.) x 4° (lat.)	T42 (~2.8° x 2.8°)
Layers (top)	15 (1 hPa)	30 (0.4 hPa)
Solar radiation	Lacis and Hansen (1974)	Shibata and Uchiyama (1992)
(SW)	H_2O, O_3	H_2O, O_3, CO_2, O_2aerosol
Long wave radiation	Shibata and Aoki (1989)	Shibata and Aoki (1989)
(LW)	H_2O, CO_2, O_3	H_2O, CO_2, O_3, CH_4, N_2O
Convection	Arakawa and Schubert (1974)	Prognostic Arakawa-Schubert
		Randall and Pan (1993)
Planetary Boundary	Bulk layer (Tokioka et al., 1988)	Mellor and Yamada (1974)
Layer (PBL)		
Gravity wave drag	Palmer et al. (1986)	Iwasaki et al. (1989)
	Rayleigh friction	Rayleigh friction
Cloud type	Penetrative convection,	Penetrative convection
	Middle-level convection,	
	Large-scale condensation,	Large-scale condensation
	stratus in PBL	
Cloudiness	Saturation	Function of relative humidity
Cloud overlap	Random for nonconsecutive clouds,	Random + correlation
	0.3 for convective clouds	
Cloud water content	Function of pressure and	Function of temperature
	temperature	
Land process	4-layer diffusion model	3-layer simple biosphere (SiB)

Feature	MRI-CGCM1	MRI-CGCM2
Oceanic component		
Horizontal resolution	2.5 ° (long) x 2 ° to 0.5 ° (lat)	
Layers (min. thickness)	21 (5.2 m)	23 (5.2 m)
Eddy viscosity	H. visc. 2.0 x 10^5 m^2s^{-1}	H. visc. 1.6 x 10^5 m^2s^{-1}
	V. visc. 1 x 10^{-4} m^2s^{-1}	V. visc. 1 x 10^{-4} m^2s^{-1}
Eddy mixing	Horizontal-vertical mixing	Isopycnal mixing
		+ Gent and McWilliams (1990)
	H. diff. 5.0 x 10^3 m^2s^{-1}	Isopycnal 2.0 x 10^3 m^2s^{-1}
	V. diff. 5.0 x 10^{-5} m^2s^{-1}	Diapycnal 1.0 x 10^{-5} m^2s^{-1}
Vertical viscosity and diffusivity	Mellor and Yamada (1974, 1982)	
Sea ice	Mellor and Kantha (1989)	
Atmosphere-ocean coupling		
Coupling interval	6 hours	24 hours
Flux adjustment	Heat, salinity	Heat, salinity + wind stress (in the equatorial band 12 ° S to 12 ° N)

IPCC SRES and Stabilization Scenarios

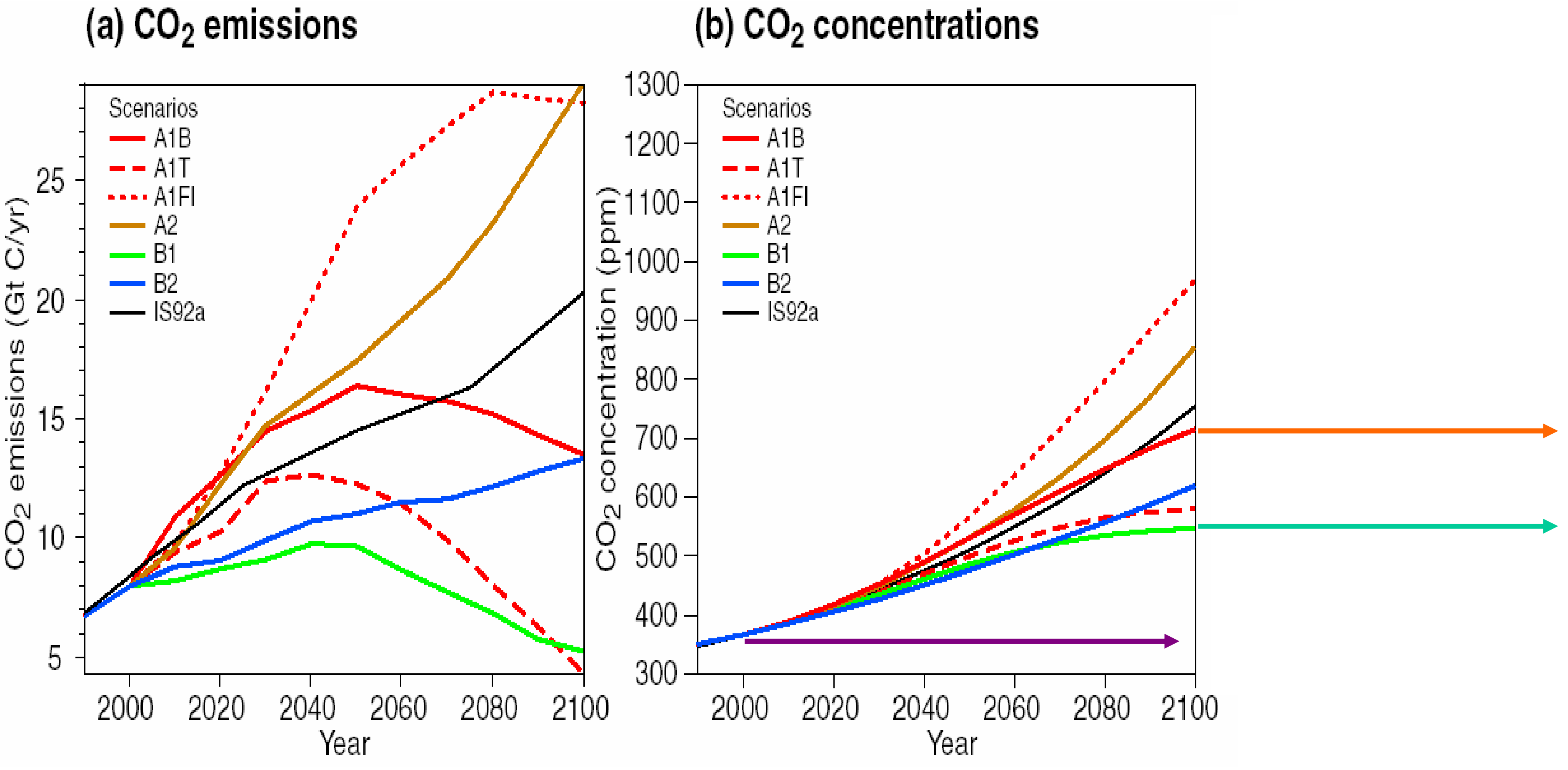

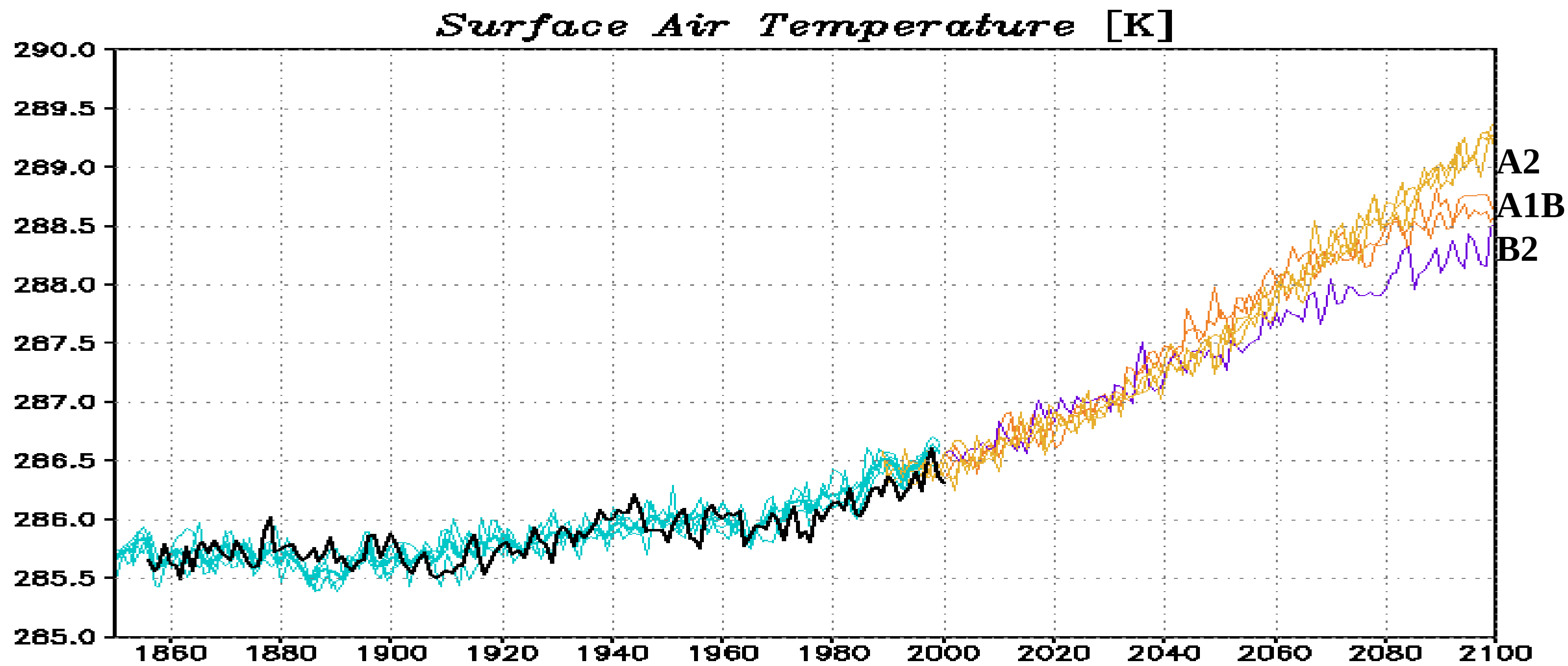
Surface Air Temperature [K]
290.0
289.5
289.0
288.5
288.0
287.5
287.0
286.5
286.0
285.5
285.0
1860
1880
1900
1920
1940
1960
1980
2000
2020
2040
2060
2080
2100
A2
A1B
B2

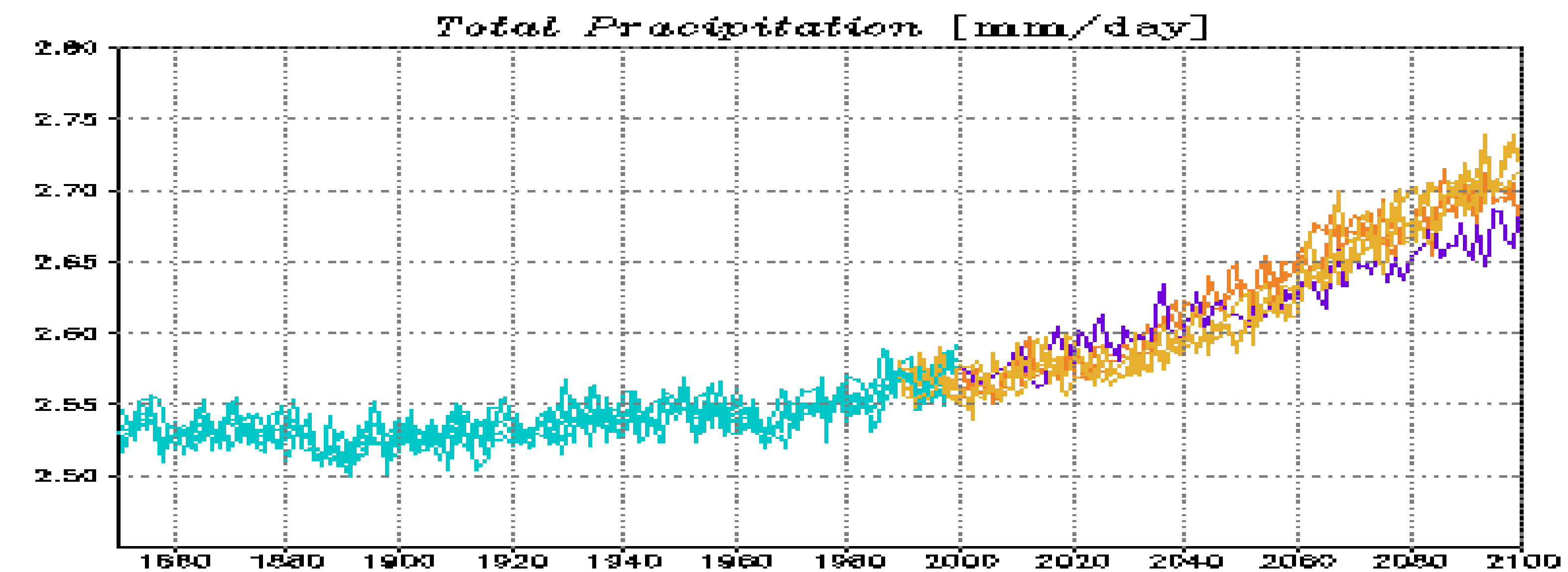
Total Precipitation [mm/day]
2.80
2.75
2.70
2.65
2.60
2.55
2.50
1860
1880
1900
1920
1940
1960
1980
2000
2020
2040
2060
2080
2100

MRI-CGCM2.3

Surface Air Temp. Change

(2071-2100) – (1961-1990)

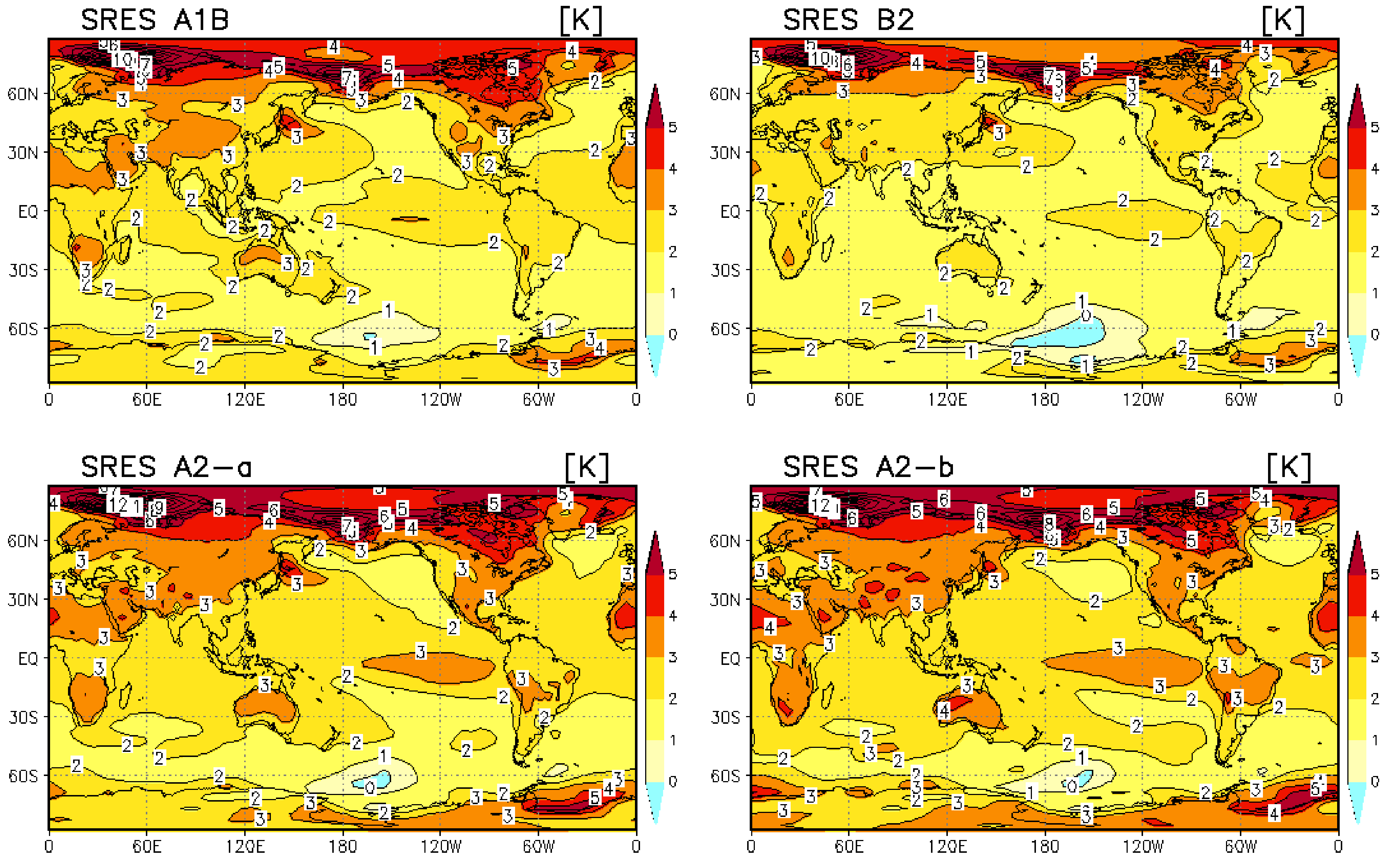

Spatial patterns of Global Warming and Natural Variability MRI-CGCM

Due to El Nino

Due to CO2 increase

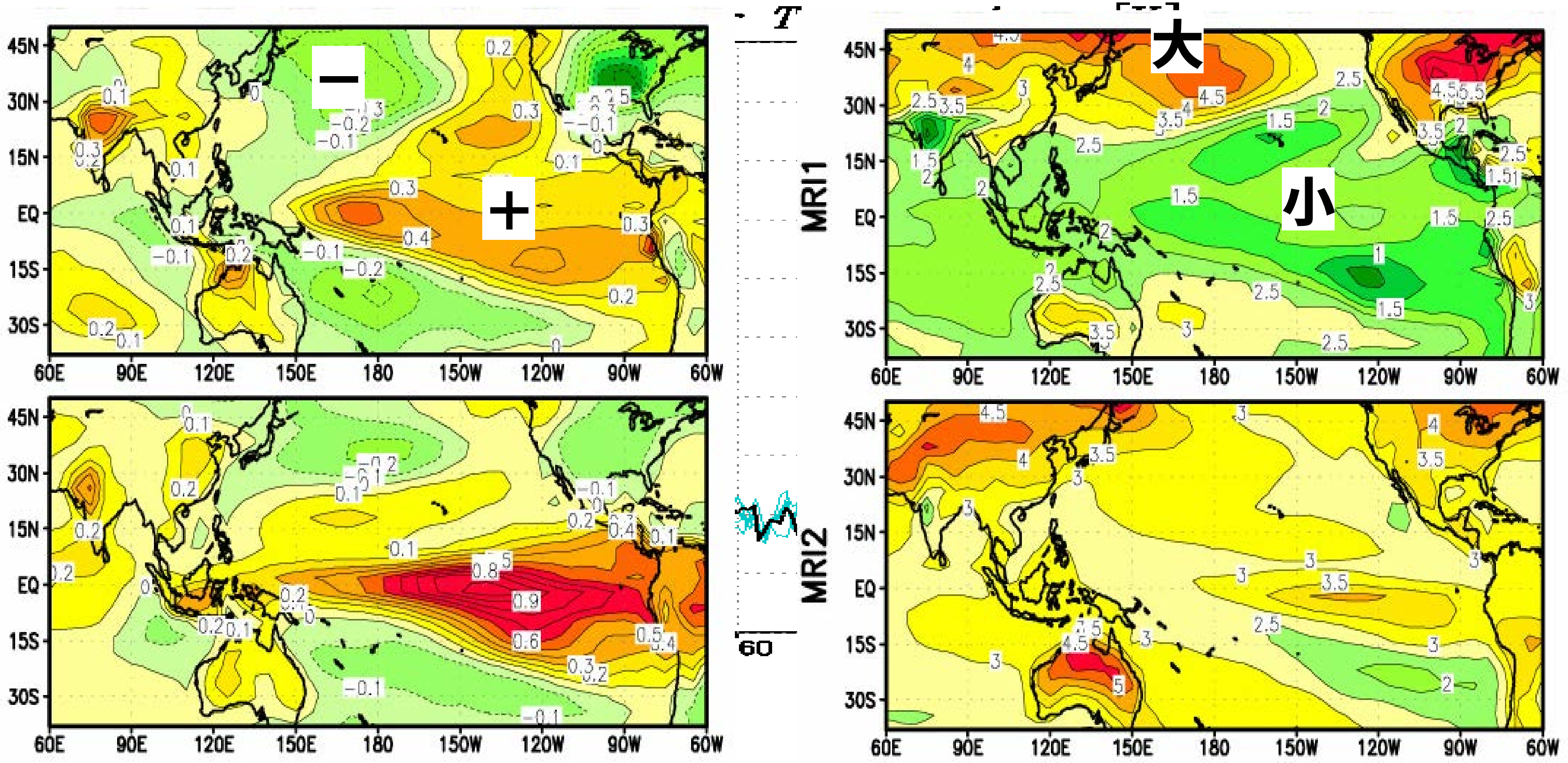

Spatial patterns of Global Warming and Natural Variability Had-CGCM

Due to El Nino **Due to CO2 increase**

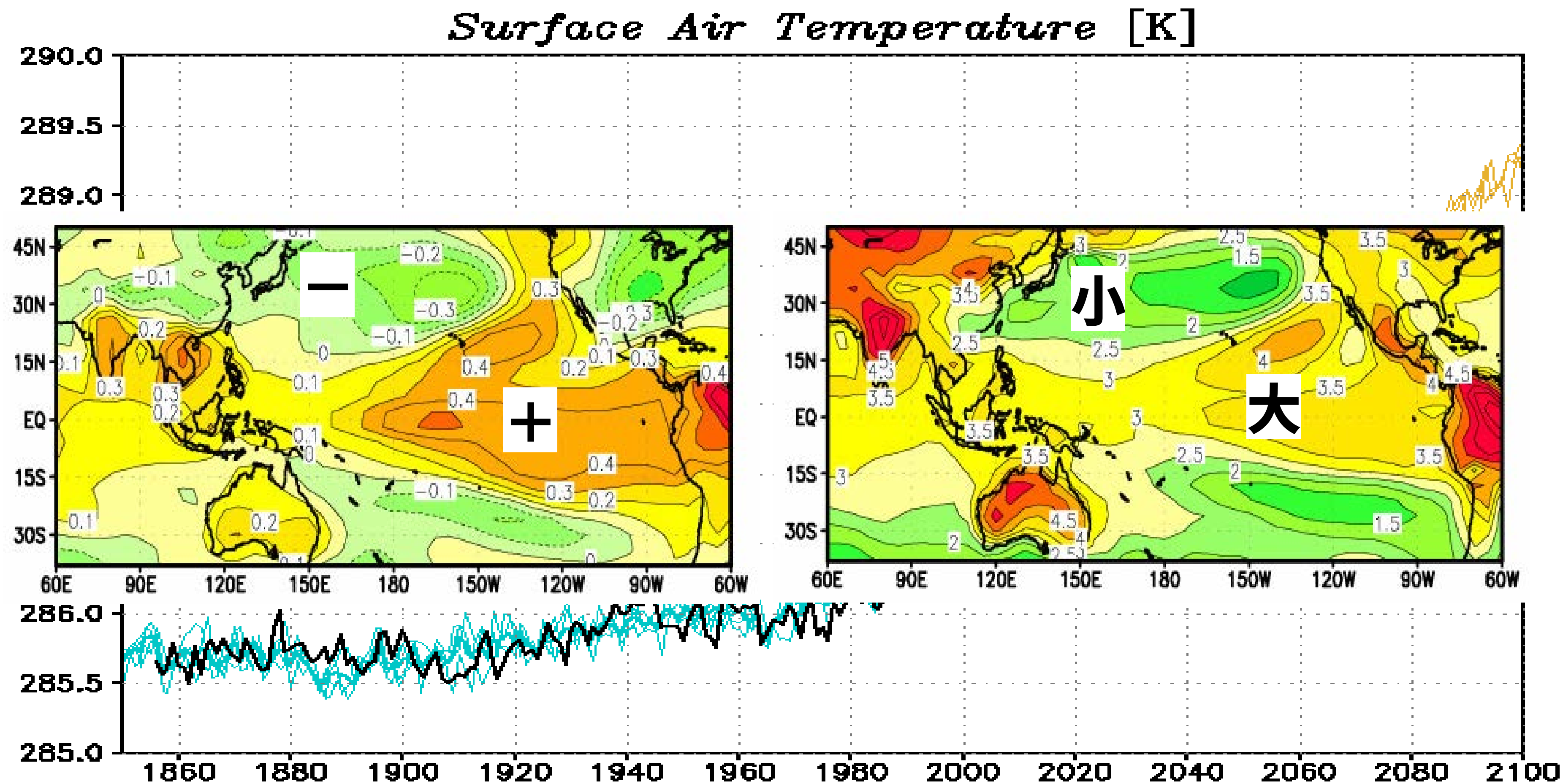

Spatial patterns of Global Warming and Natural Variability GFDL-CGCM

Due to El Nino

Due to CO2 increase

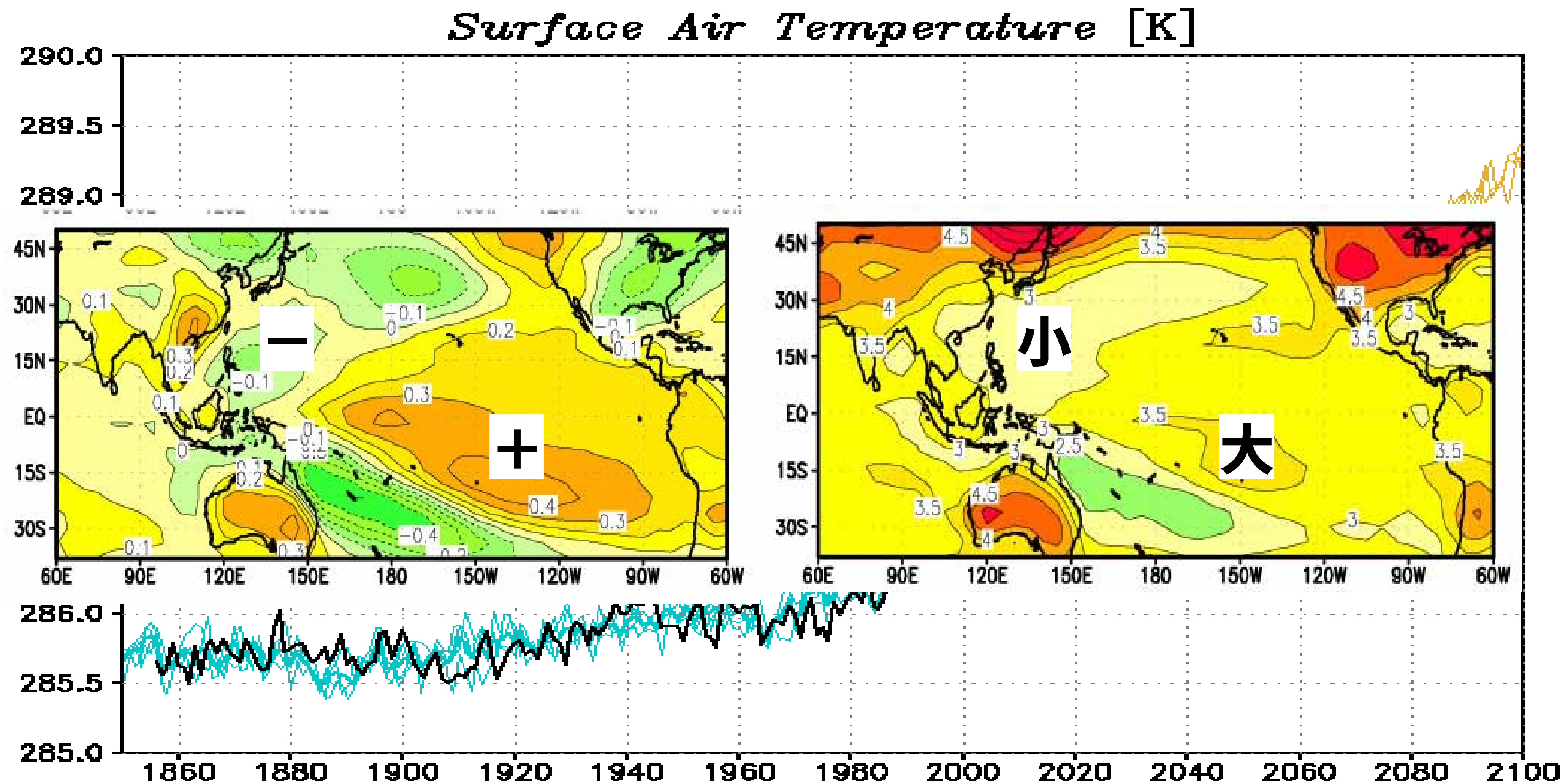

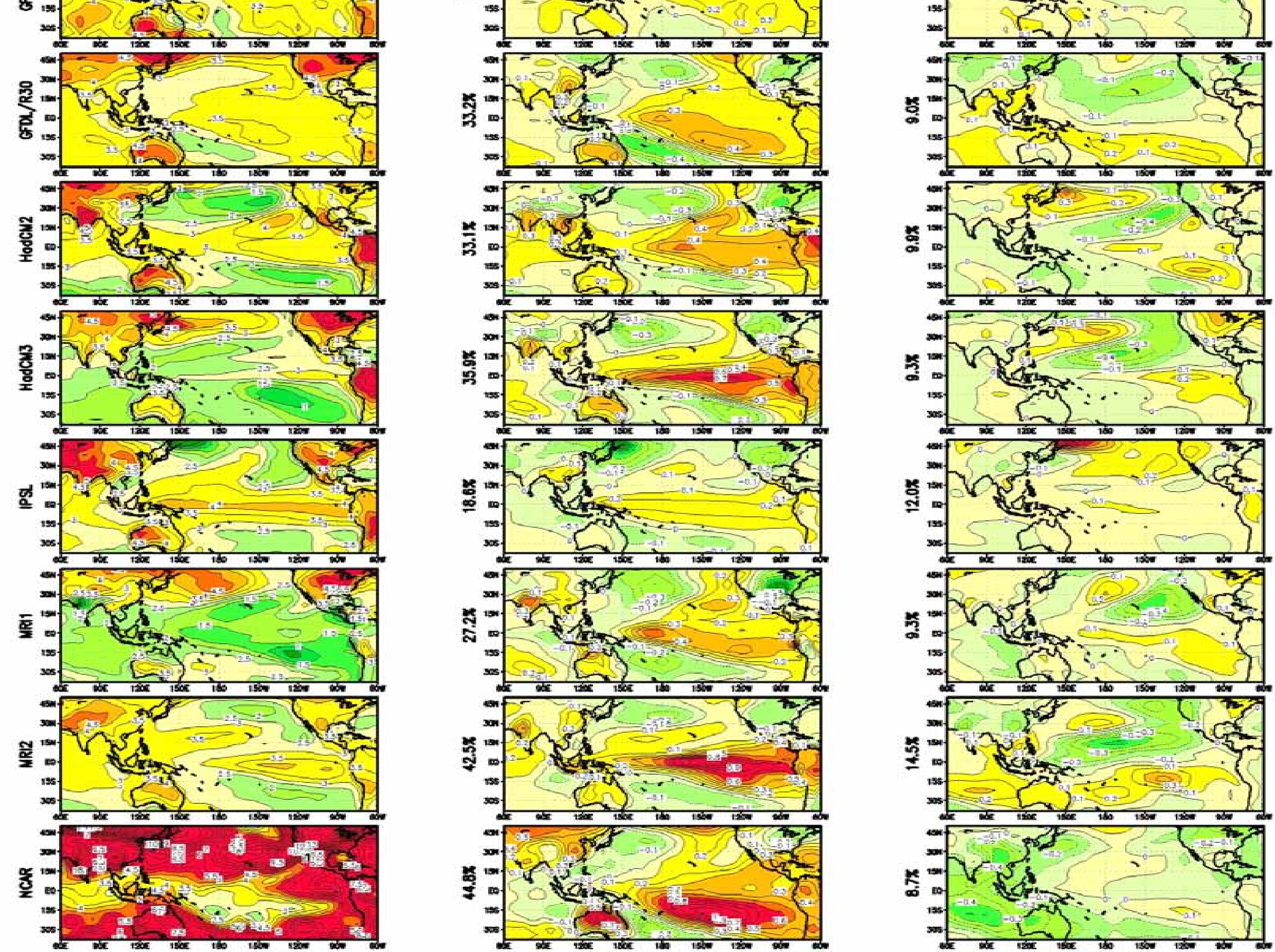
GFDL/R30
33.2%
9.0%
HadCM2
33.1%
9.9%
HadCM3
35.9%
9.3%
IPSL
18.6%
12.0%
MRI1
27.2%
9.3%
MRI2
42.5%
14.5%
NCAR
44.8%
8.7%

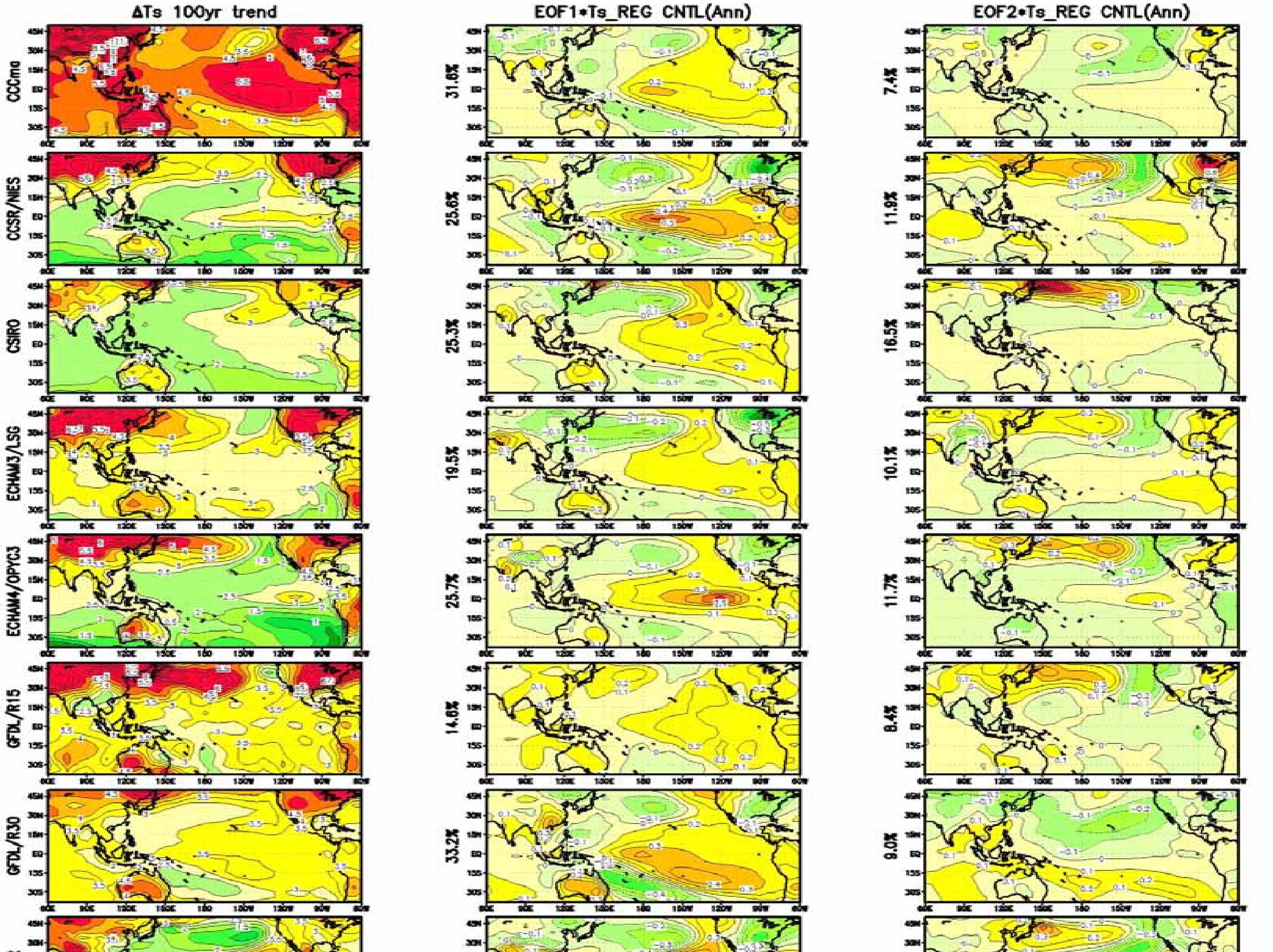
ΔTs 100yr trend
EOF1*Ts_REG CNTL(Ann)
EOF2*Ts_REG CNTL(Ann)
CCCma
31.6%
7.4%
CCSR/NIES
25.6%
11.9%
CSIRO
25.3%
16.5%
ECHAM3/LSG
19.5%
10.1%
ECHAM4/OPYC3
25.7%
11.7%
GFDL/R15
14.6%
8.4%
GFDL/R30
33.2%
9.0%

Mechanism of ENSO-like Change

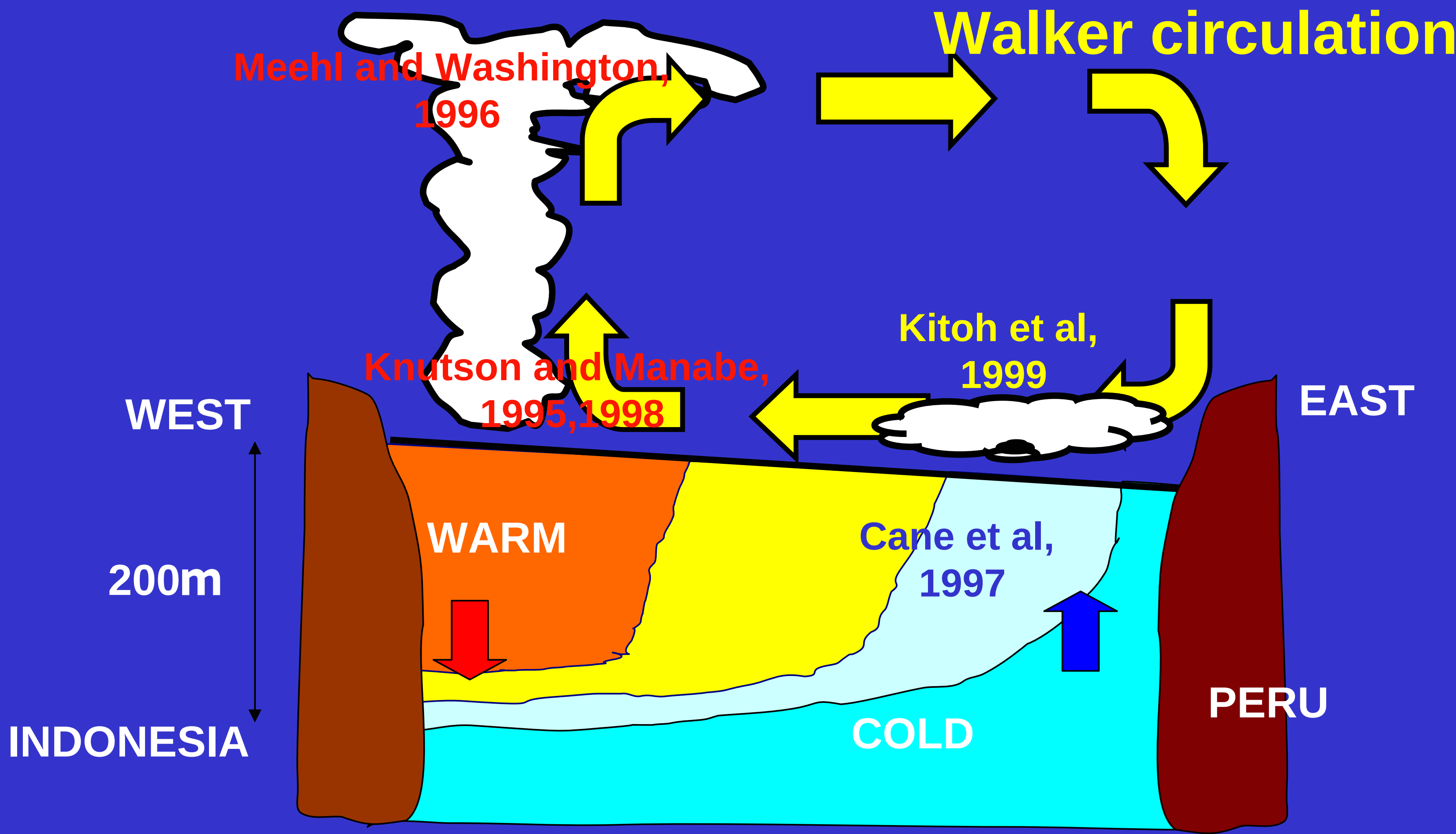

Mechanism of ENSO ⟷ ENSO-like Change

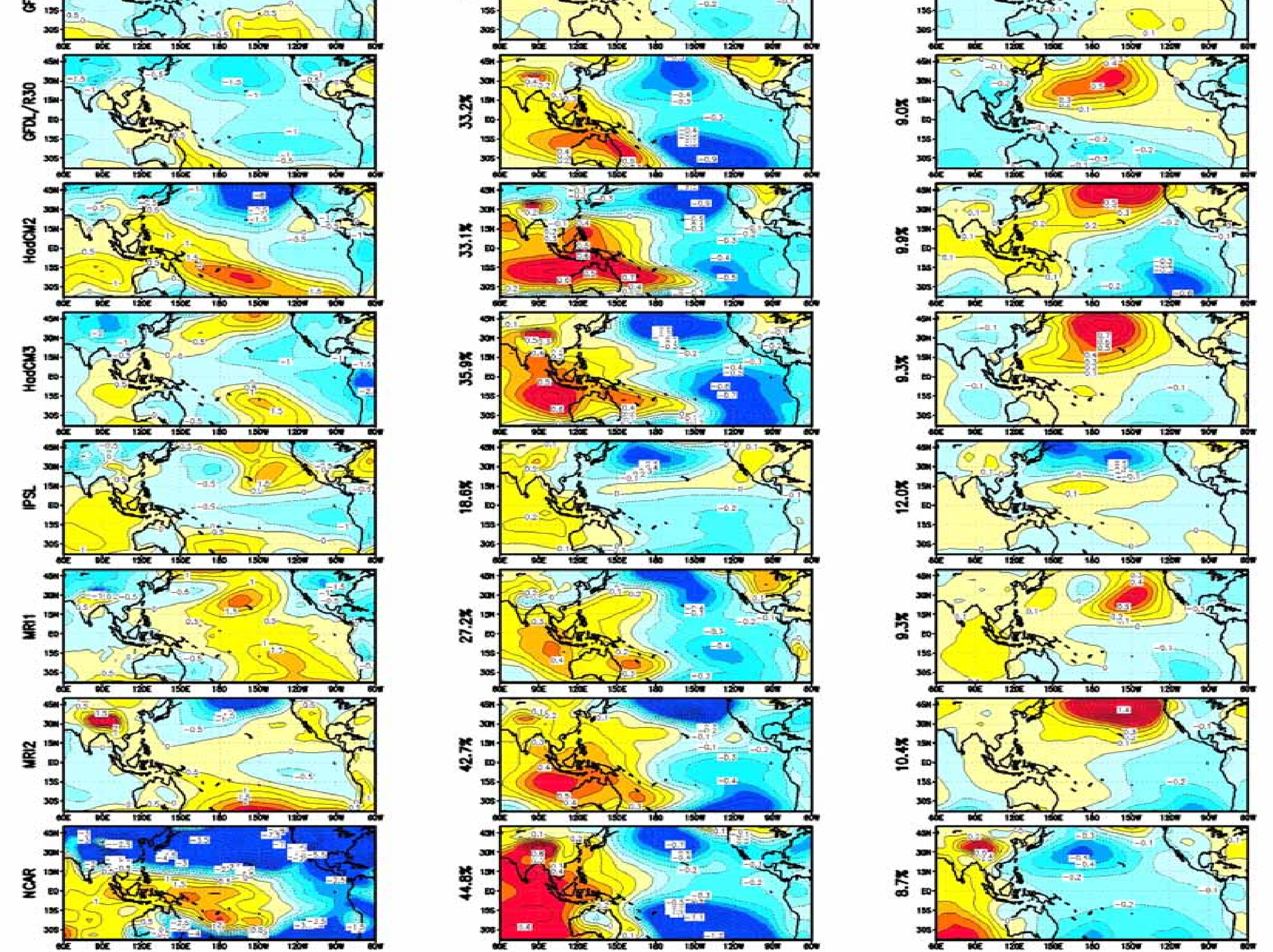

GFDL/R30
33.2%
9.0%
HadCM2
33.1%
9.9%
HadCM3
35.9%
9.3%
IPSL
18.6%
12.0%
MRI1
27.2%
9.3%
MRI2
42.7%
10.4%
NCAR
44.8%
8.7%

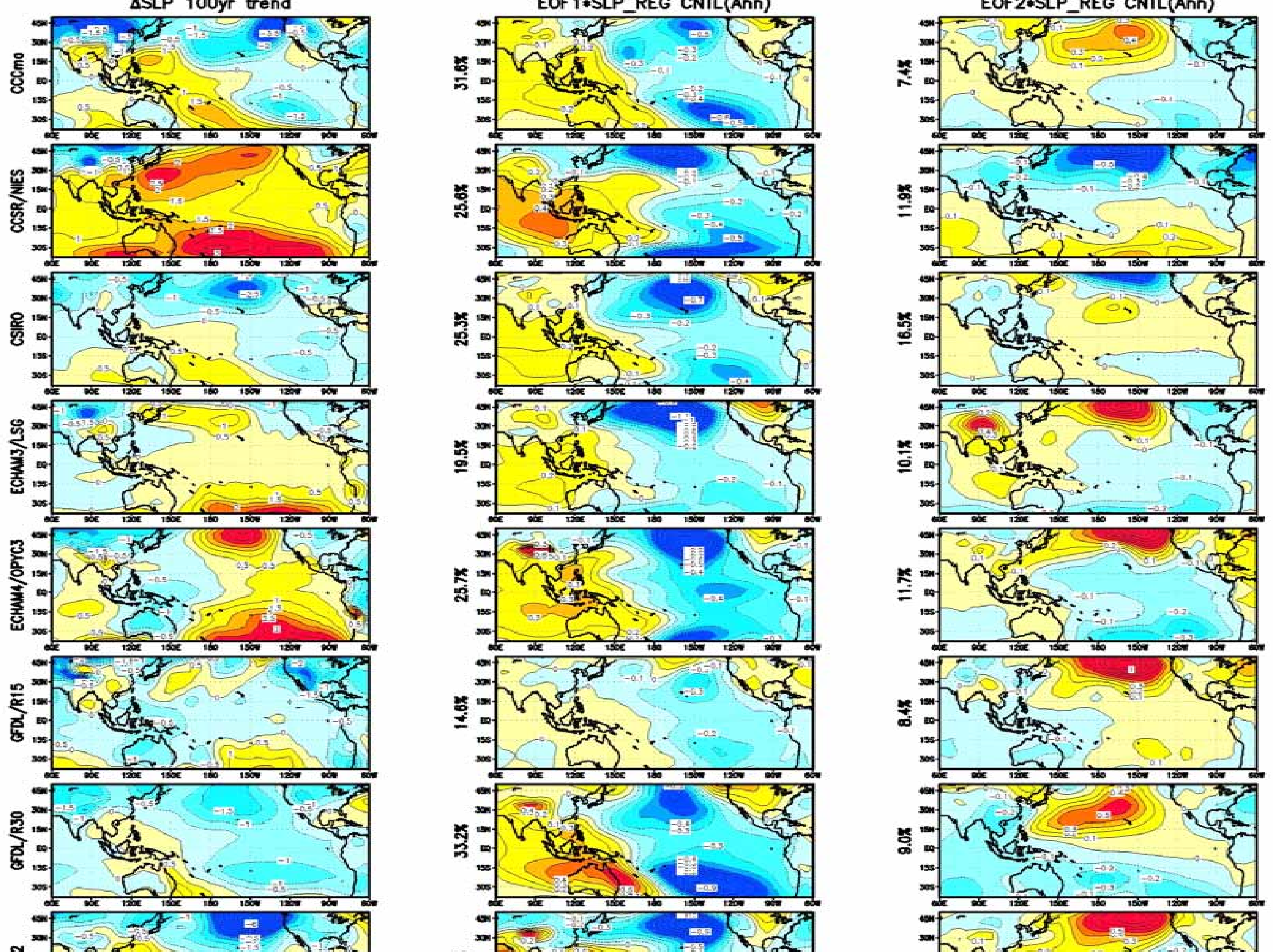
ΔSLP 100yr trend
EOF1*SLP_REG CNTL(Ann)
EOF2*SLP_REG CNTL(Ann)
CCCma
31.6%
7.4%
CCSR/NIES
25.6%
11.9%
CSIRO
25.3%
16.5%
ECHAM3/LSG
19.5%
10.1%
ECHAM4/OPYC3
25.7%
11.7%
GFDL/R15
14.6%
8.4%
GFDL/R30
33.2%
9.0%

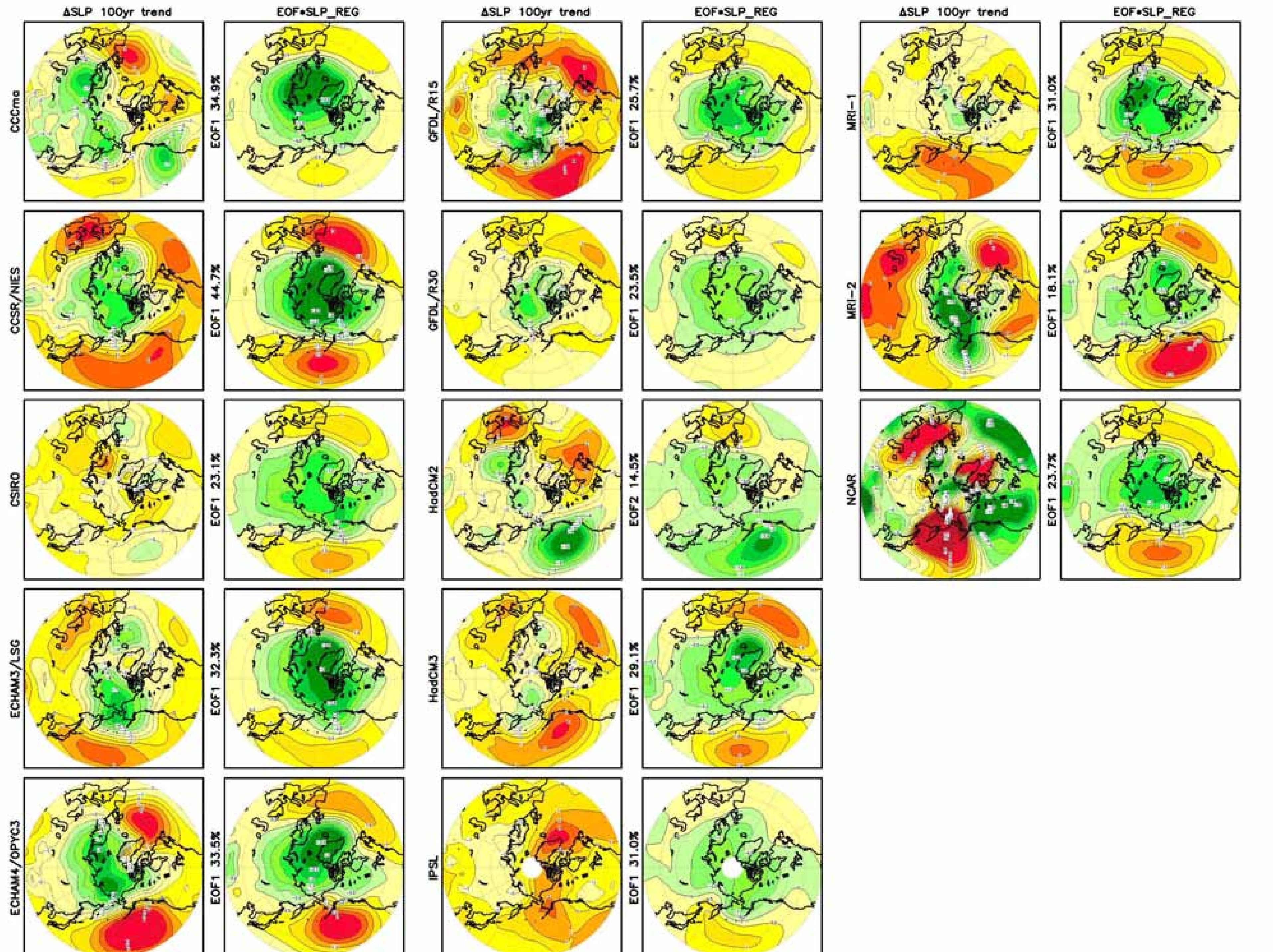
ΔSLP 100yr trend
EOF•SLP_REG
ΔSLP 100yr trend
EOF•SLP_REG
ΔSLP 100yr trend
EOF•SLP_REG
CCCma
EOF1 34.9%
GFDL/R15
EOF1 25.7%
MRI-1
EOF1 31.0%
CCSR/NIES
EOF1 44.7%
GFDL/R30
EOF1 23.5%
MRI-2
EOF1 18.1%
CSIRO
EOF1 23.1%
HadCM2
EOF2 14.5%
NCAR
EOF1 23.7%
ECHAM3/LSG
EOF1 32.3%
HadCM3
EOF1 29.1%
ECHAM4/OPYC3
EOF1 33.5%
IPSL
EOF1 31.0%

Mechanism of AO-like Change

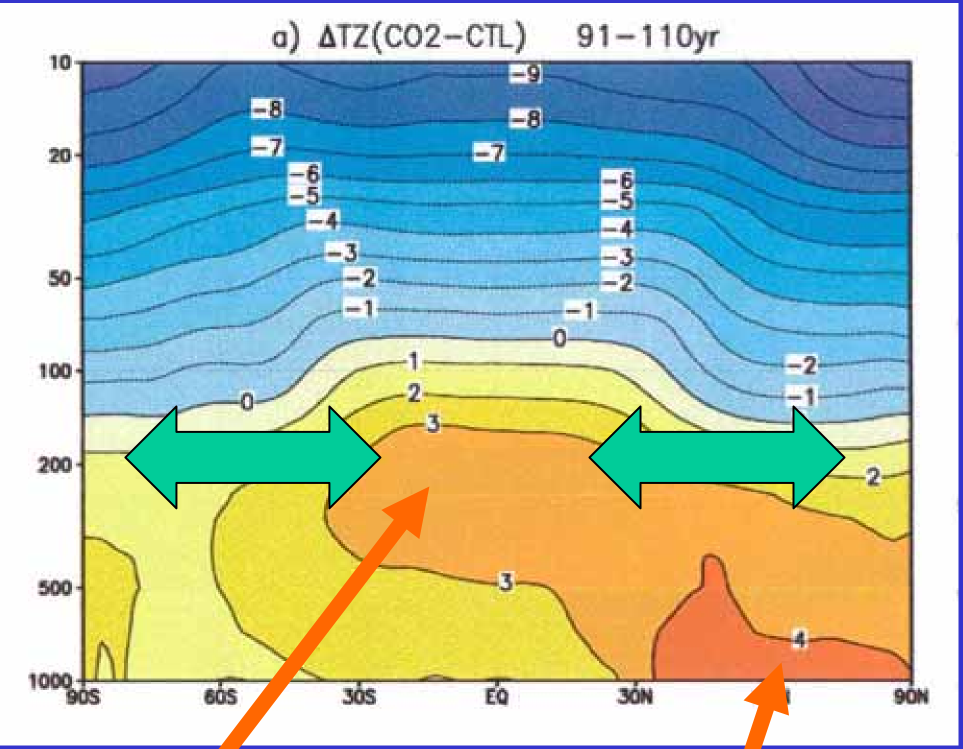

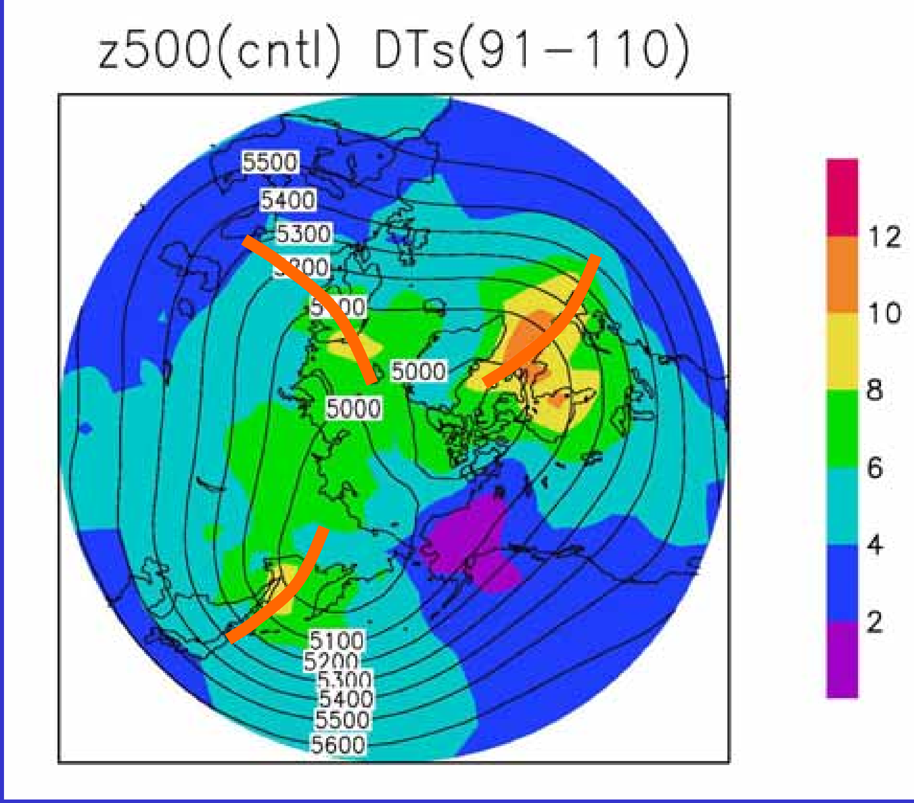

Temp. dependence of moist adiabaitic laps rate

snow-ice melt stable stratification

stronger snow/albedo feedback near the troughs

Manabe and Wetherald (1975)

Noda et al. (1996)

Possible global warming patterns suggested by CGCMs

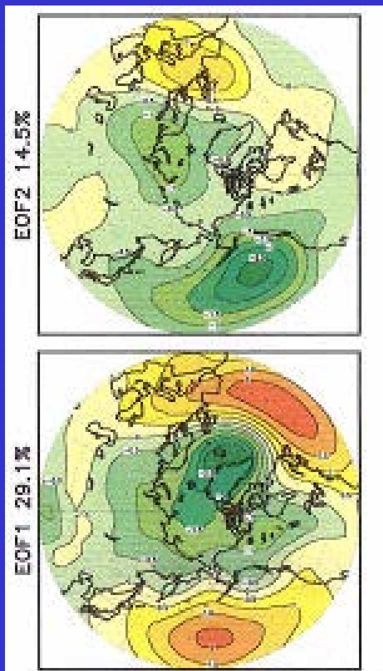

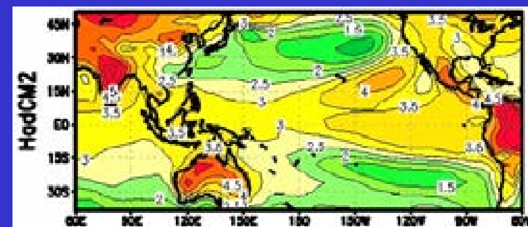

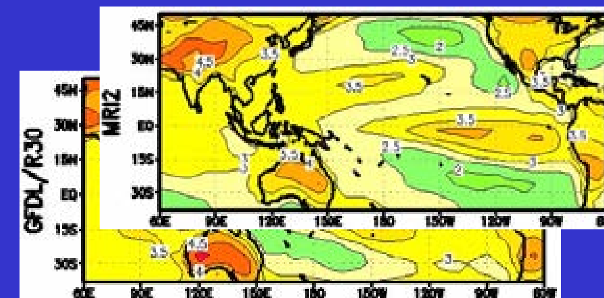

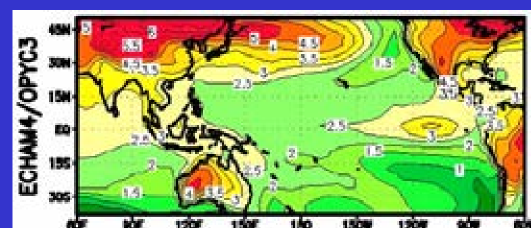

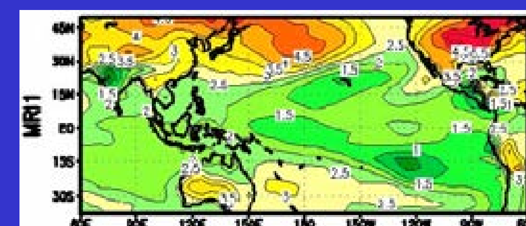

Observed trend

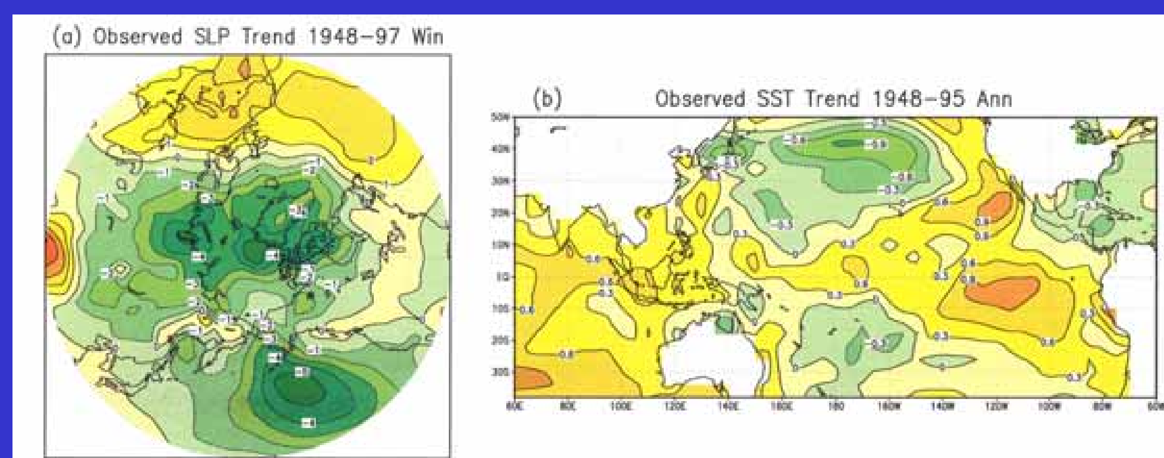

Comparison between Simulated AO-like and ENSO-like Changes

	El Niño	El Niño SO ?	El Niño SO: La Niña	La Niña
AO		CCSR/NIES HadCM3	ECHAM3/LSG ECHAM4/OPYC3 GFDL15	MRI1
Non-AO	CCCma CSIRO GFDL/R30 HadCM2 IPSL MRI2 NCAR			

Climate Modeling at MRI

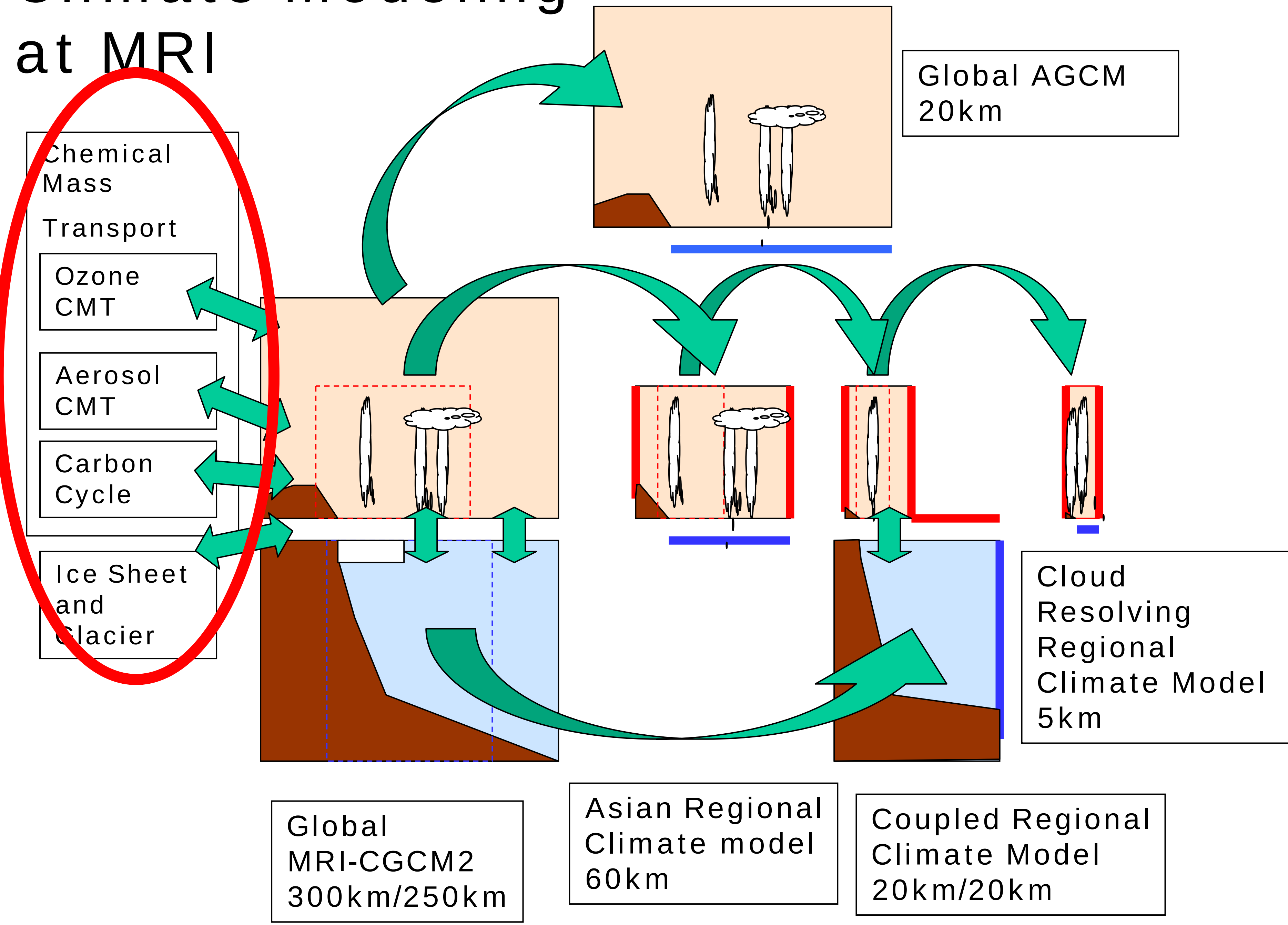

Carbon Cycle Model (included in MRI-CGCM)

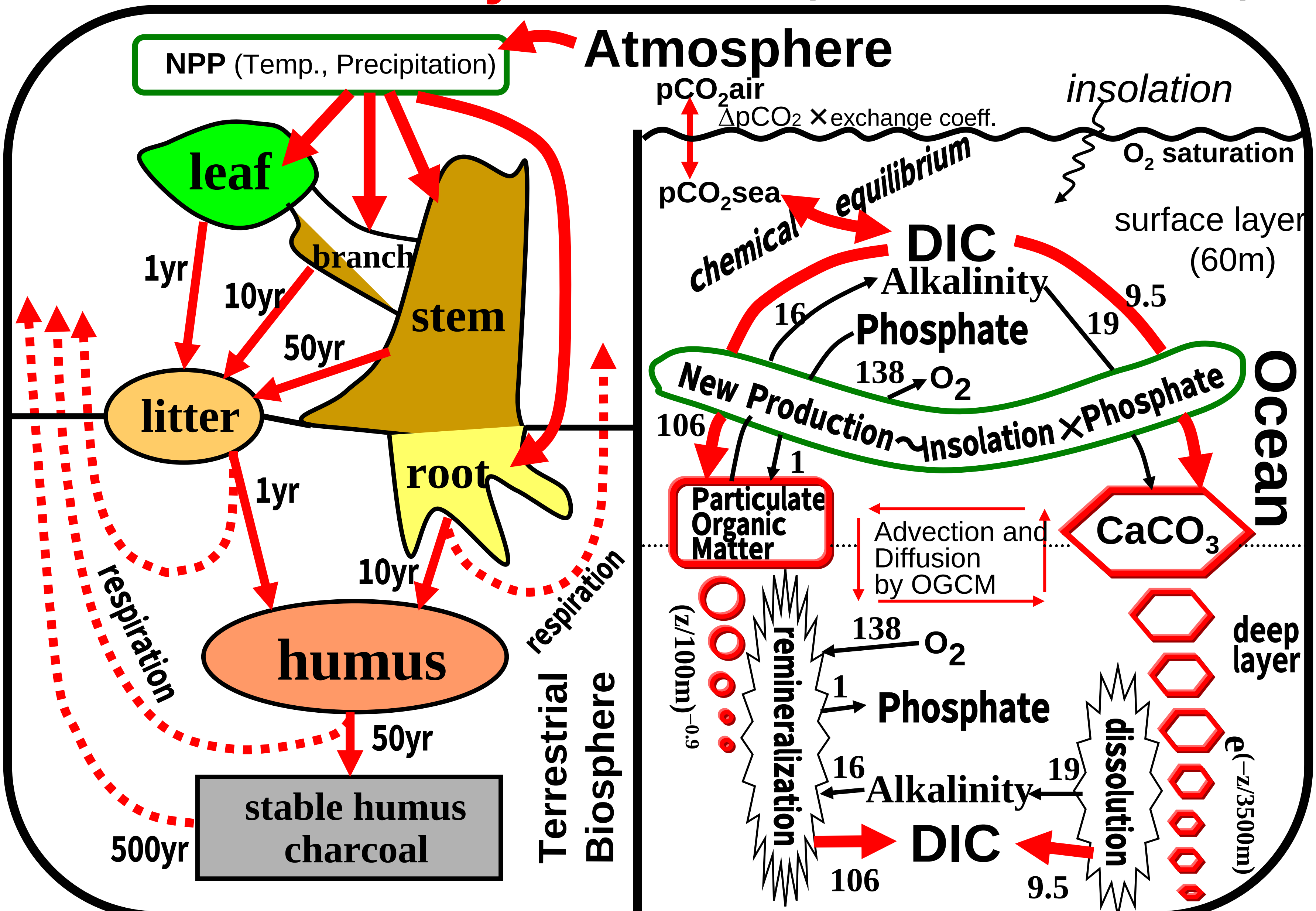

Terrestrial Biosphere Model follows Goudriaan and Ketner (1984).
NPP (Miami model: Lieth (1975), Friedlingstein et al. (1992)).

Ocean model by Obata (2001) and Obata and Kitamura (2003)

気象研海洋炭素循環モデルによる海洋大気間二酸化炭素交換の経年変動(1961-1998)

Ocean Carbon Cycle Model
by Meteorological Research Institute

Climate change experiment 1961-1998 (driven by NCEP wind and JMA SST)

Figure:
Sea-to-Air CO_2 flux (in GtC/year)

dashed line: global (variability (1std) = 0.23 GtC/yr)
solid thick line: each region

Equatorial eastern Pacific (0.13 GtC/yr) is dominant by the ENSO (during El Niño, weak easterly, weak upwelling, reduced carbon supply from deeper waters and reduced sea-air CO_2 flux).

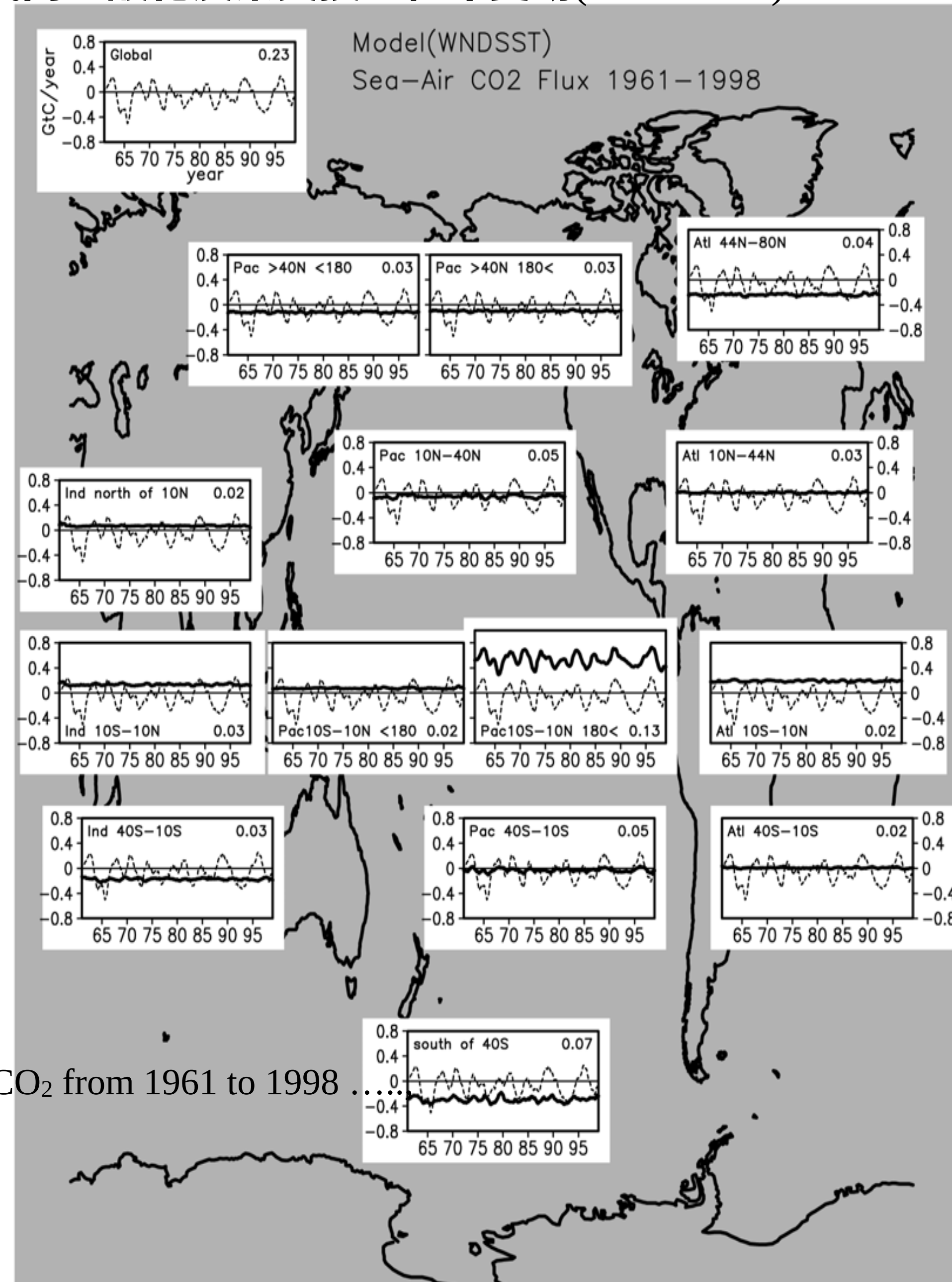

Obata and Kitamura,
Interannual variability of the sea-air exchange of CO_2 from 1961 to 1998 ….
J. Geophys. Res., 108 (C11), 2003.

Net Primary Production

(empirically determined from temperature andprecipitation, including pCO_2air fertilization effect)

MRI model in 1976

(pCO2air = 315ppm)

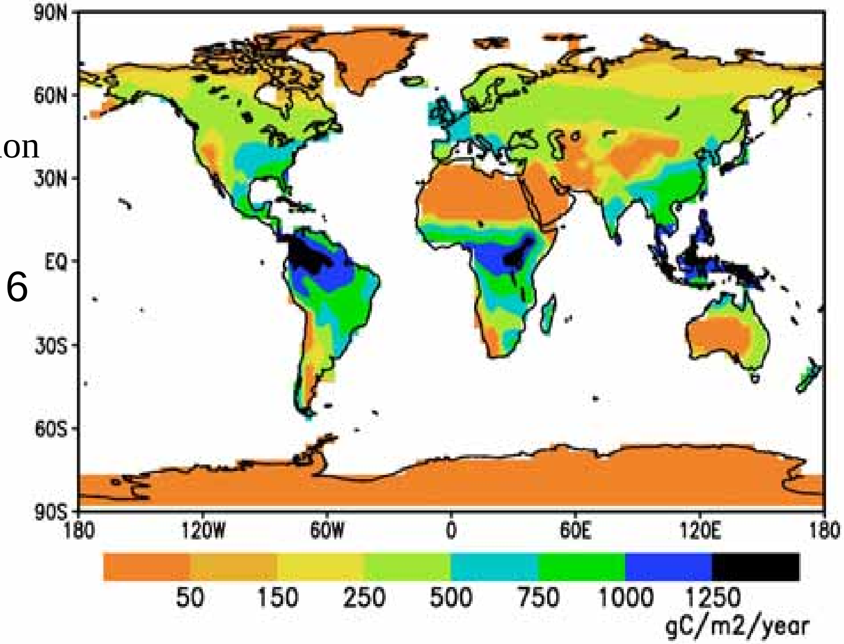

Global amount = 58 GtC/year

More detailed model

Woodward et al. (GBC, 1995)

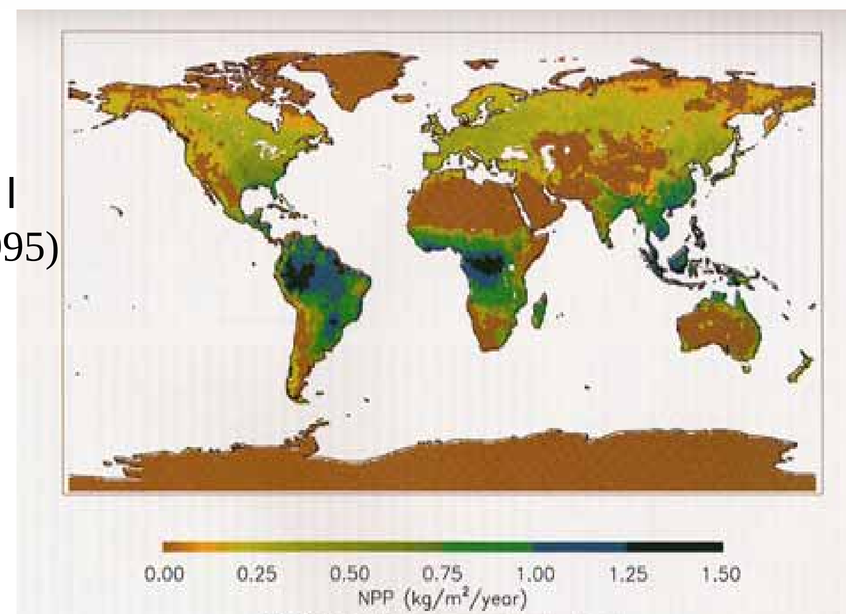

Plate 2. Global distribution of annual net primary productivity.

Global warming experiment using Fossil Fuel CO_2 Emission (IS92a scenario 1999-2100)

Emission: CDIAC(1850-1998), IS92a(1999-2100). (N_2O, CH_4, Halocarbon, tropos. Ozone: IS92a concentration)

Initial (1850)
Atmos 592 GtC
Ocean 36343 GtC
Land 2412 GtC

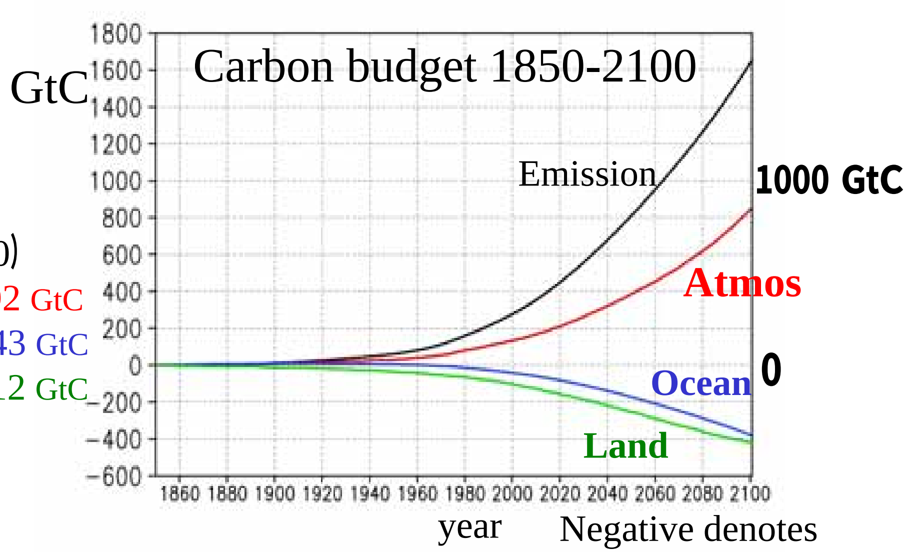

Negative denotes increase for ocean and land.

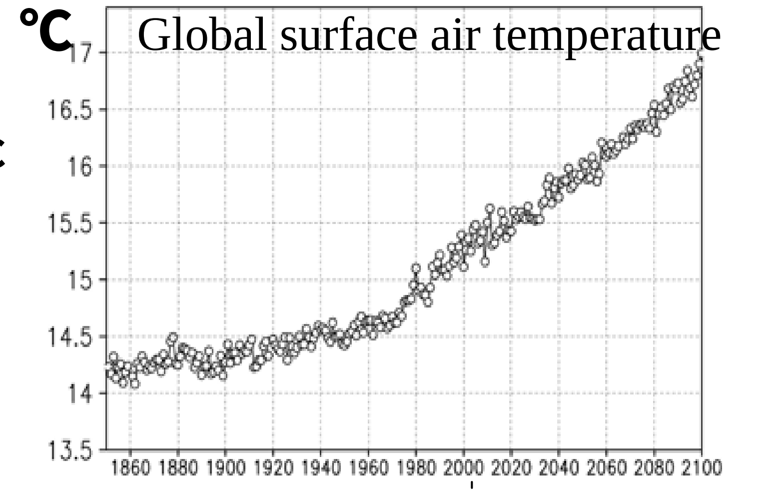

Warming of 1°C → Warming of 1.5°C

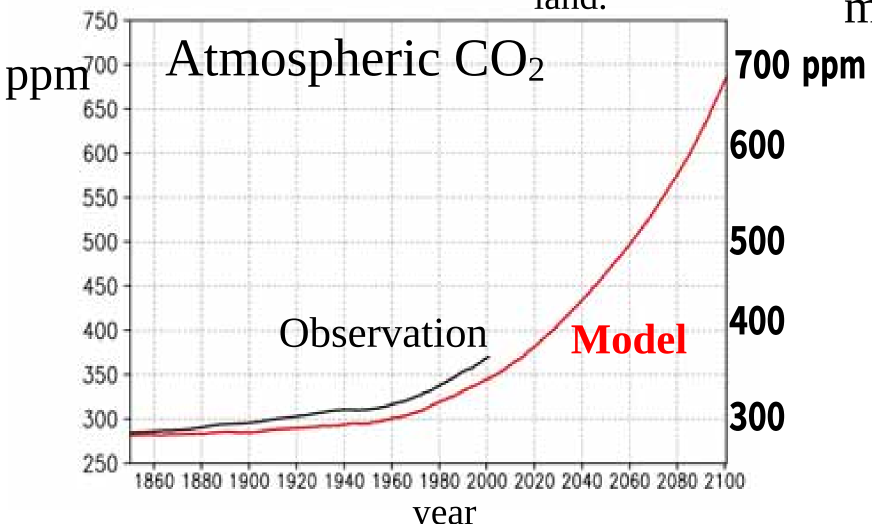

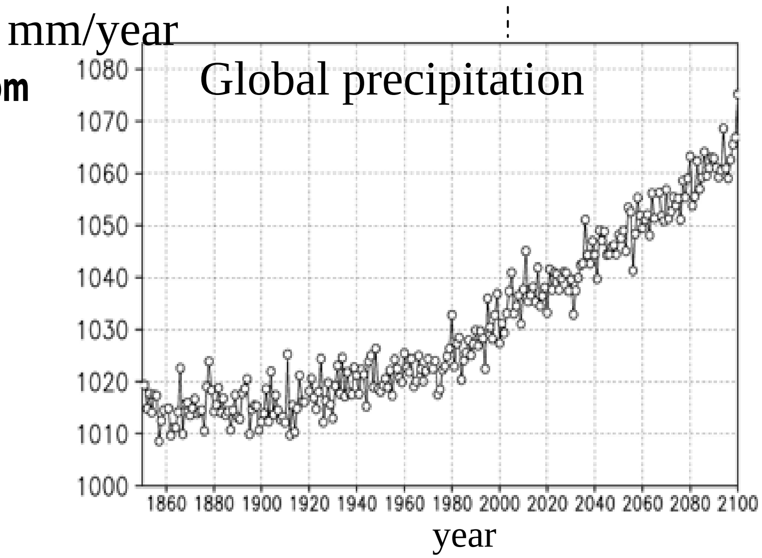

CO_2 to the atmosphere from land-use change (e.g., 124 GtC: 1850-1990) is **not** included.

Global warming experiment (IS92a CO_2 emission)

Atlantic Meridional Circulation related to NADW formation

(Contour interval = $2\times10^6 m^3/s$)

Year: 1860

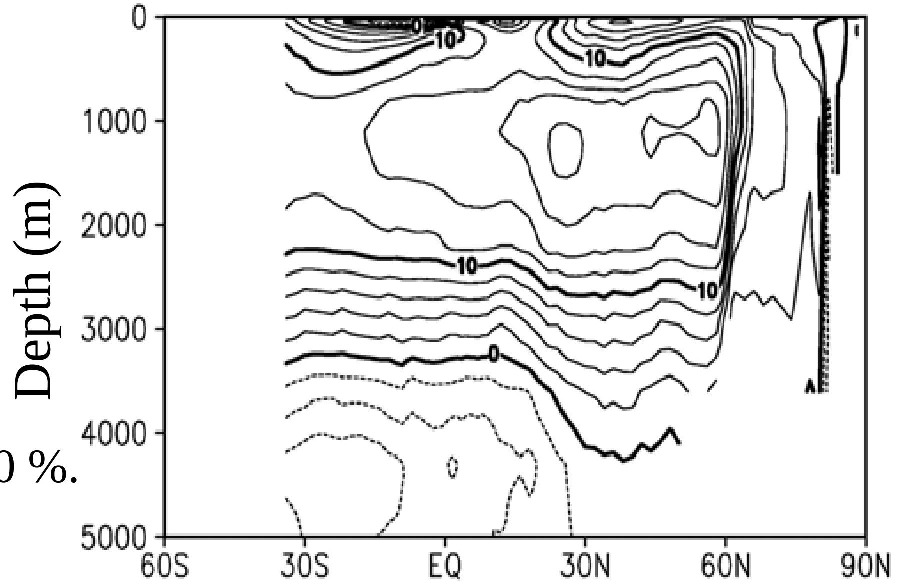

NADW is reduced by 20 %.

18Sv

↓

14Sv

Year: 2100

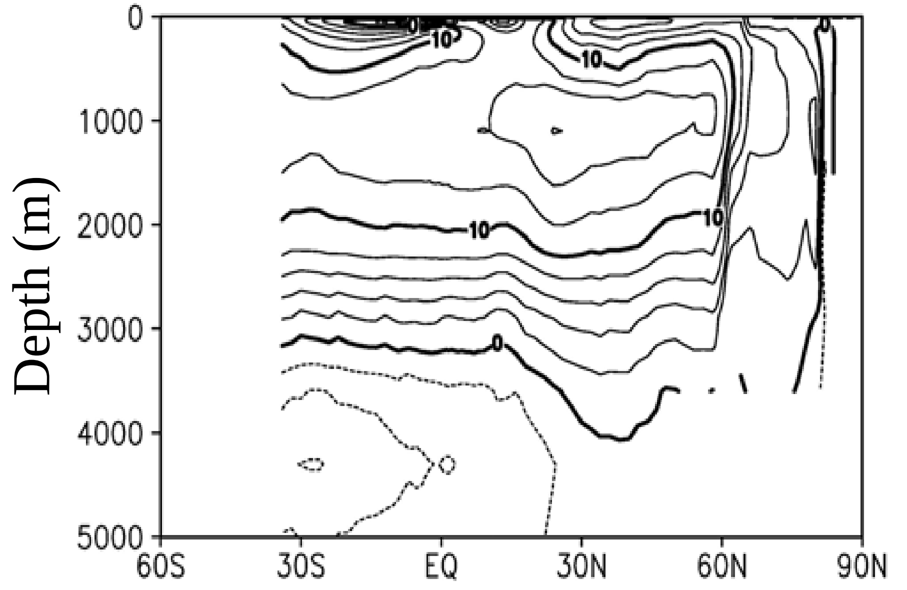

Climate Modeling at MRI

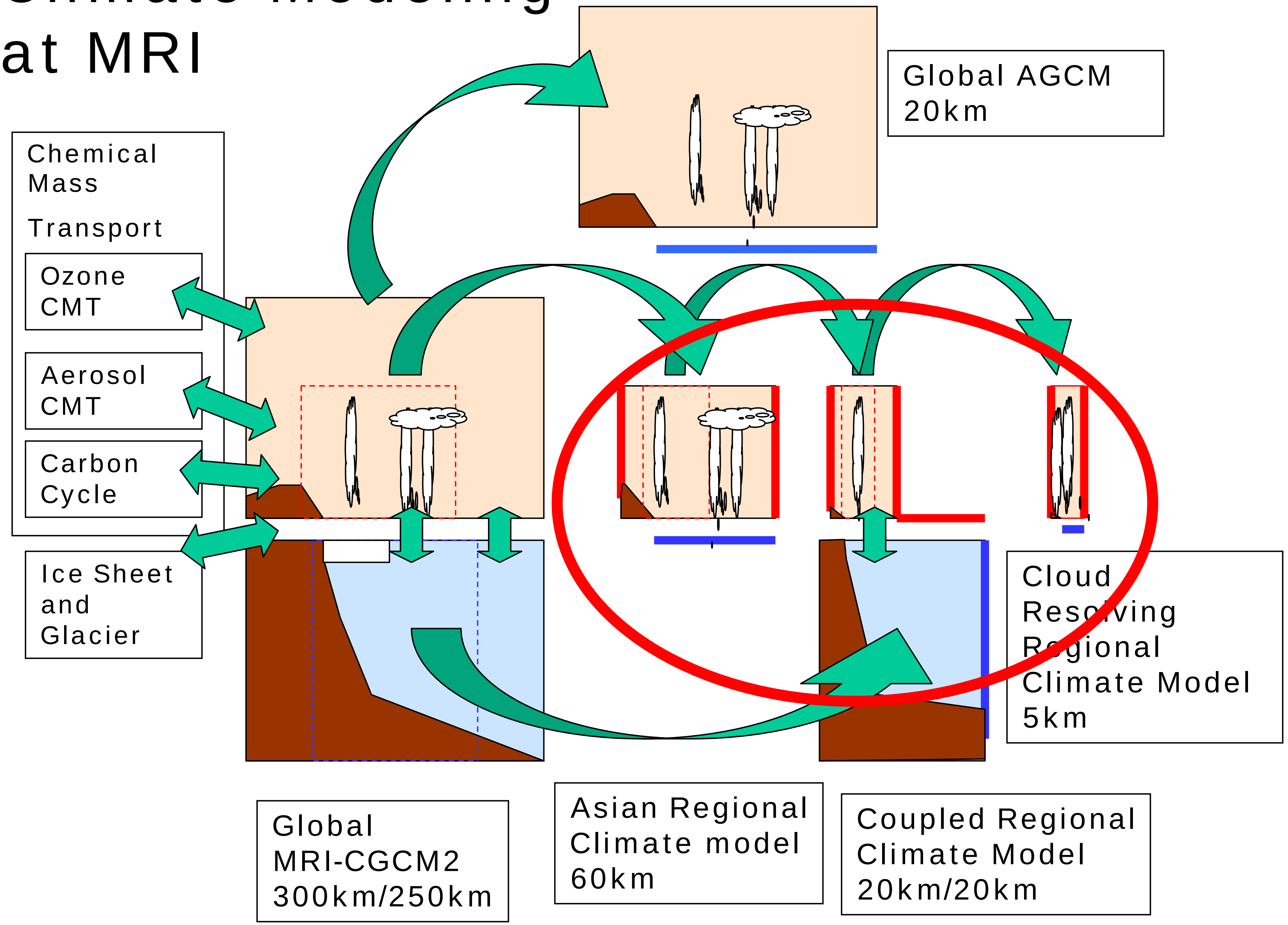

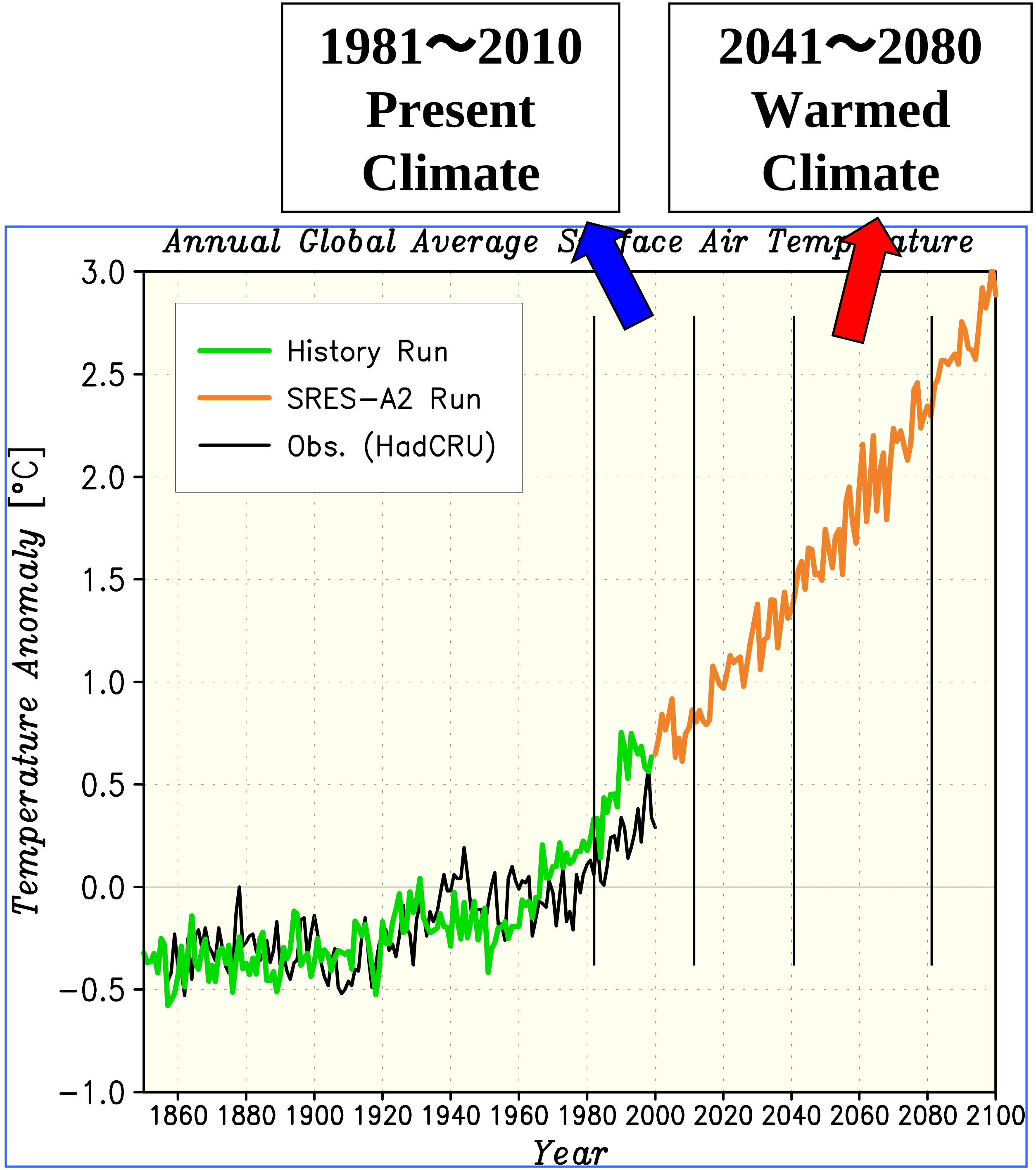
1981〜2010
Present
Climate
2041〜2080
Warmed
Climate
Annual Global Average Surface Air Temperature
History Run
SRES−A2 Run
Obs. (HadCRU)
Temperature Anomaly [°C]
3.0
2.5
2.0
1.5
1.0
0.5
0.0
−0.5
−1.0
1860 1880 1900 1920 1940 1960 1980 2000 2020 2040 2060 2080 2100
Year

Annual mean SST

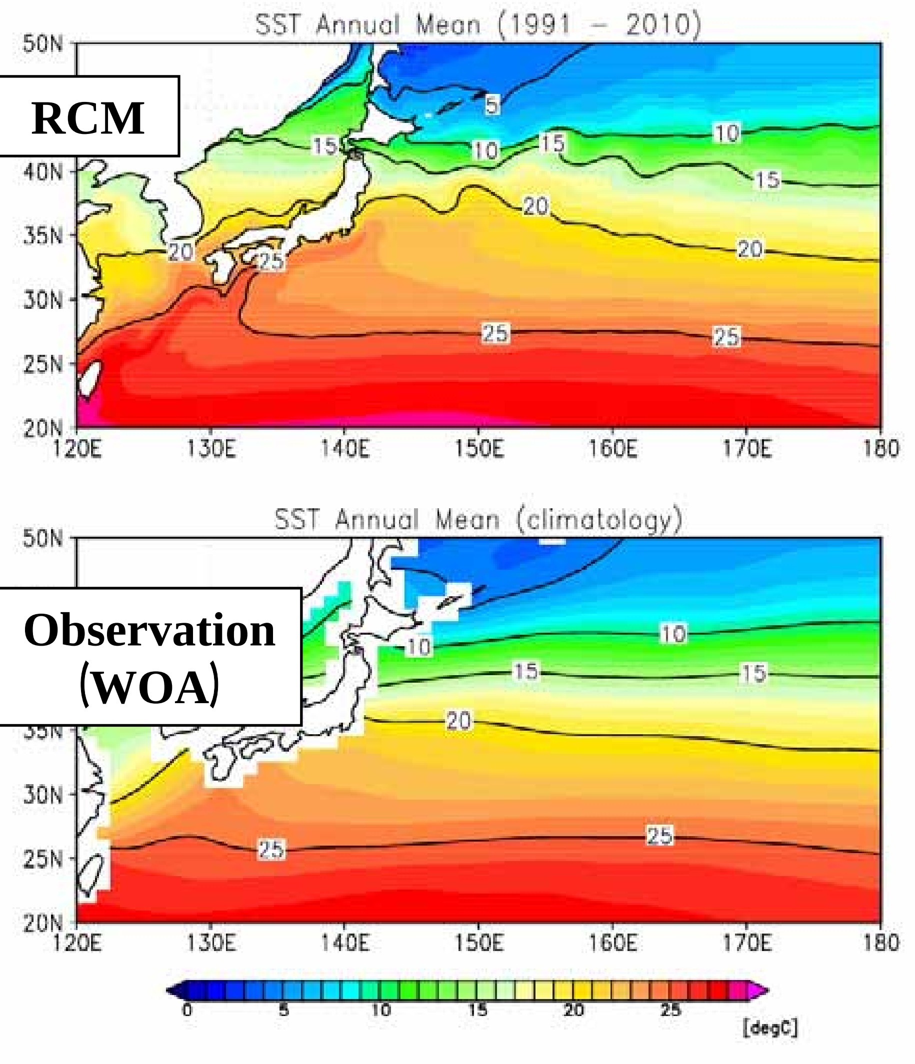

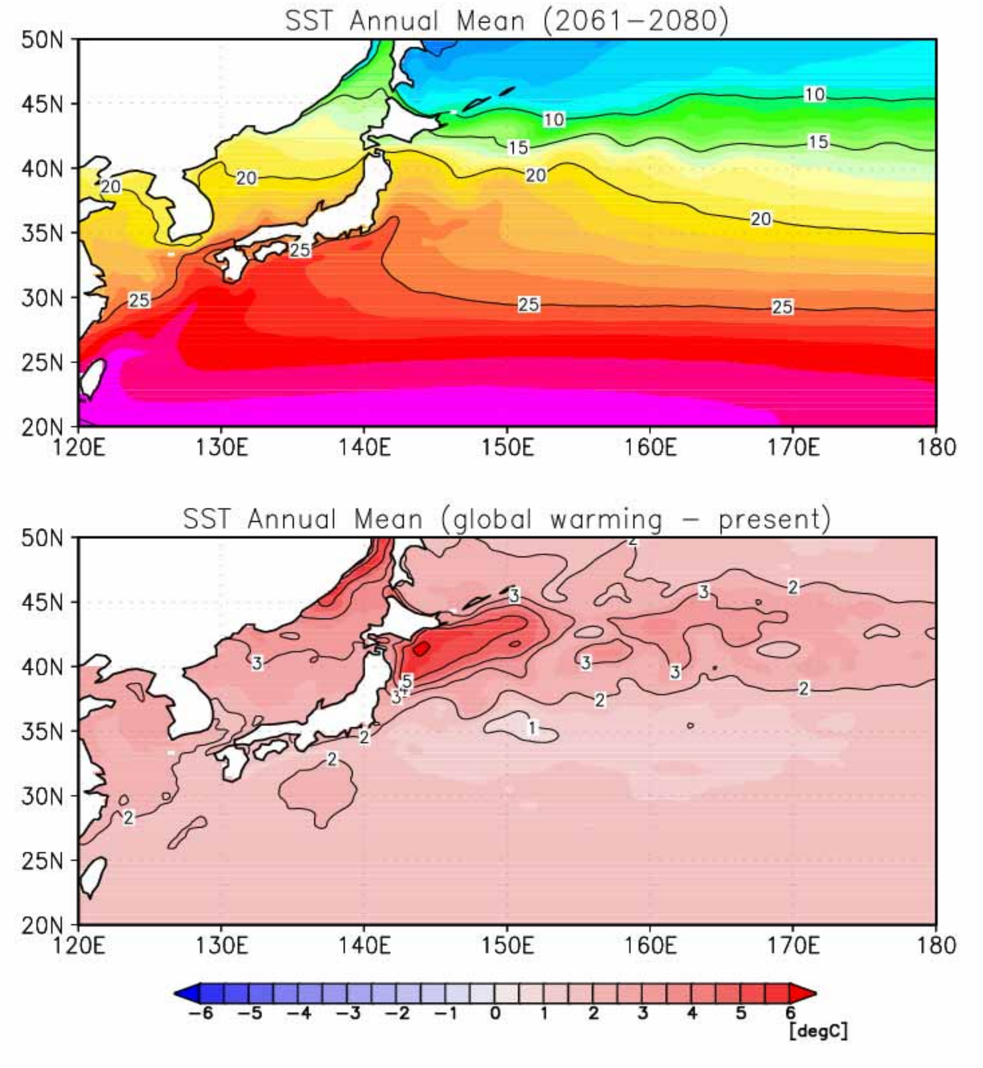

Dynamical sea level height (cm)

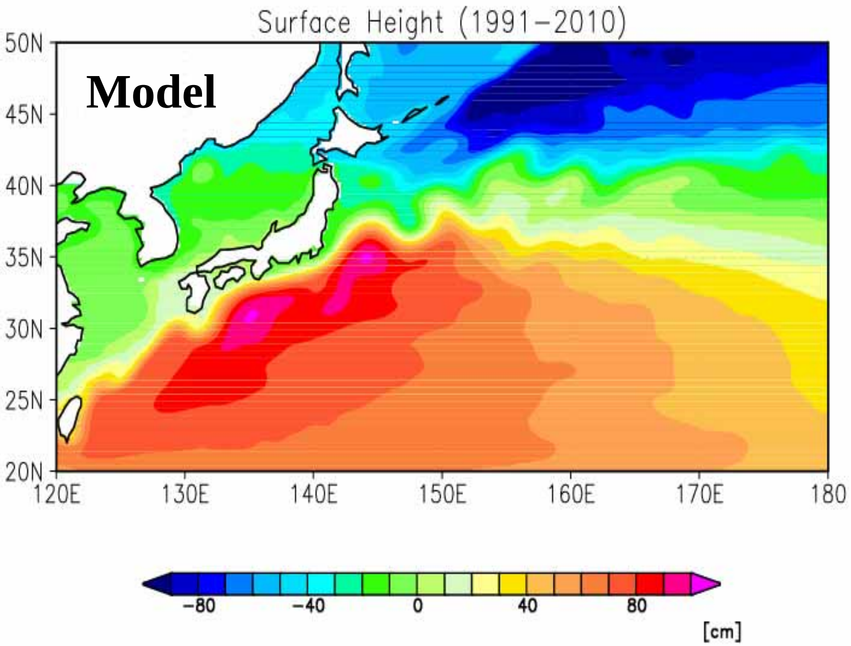

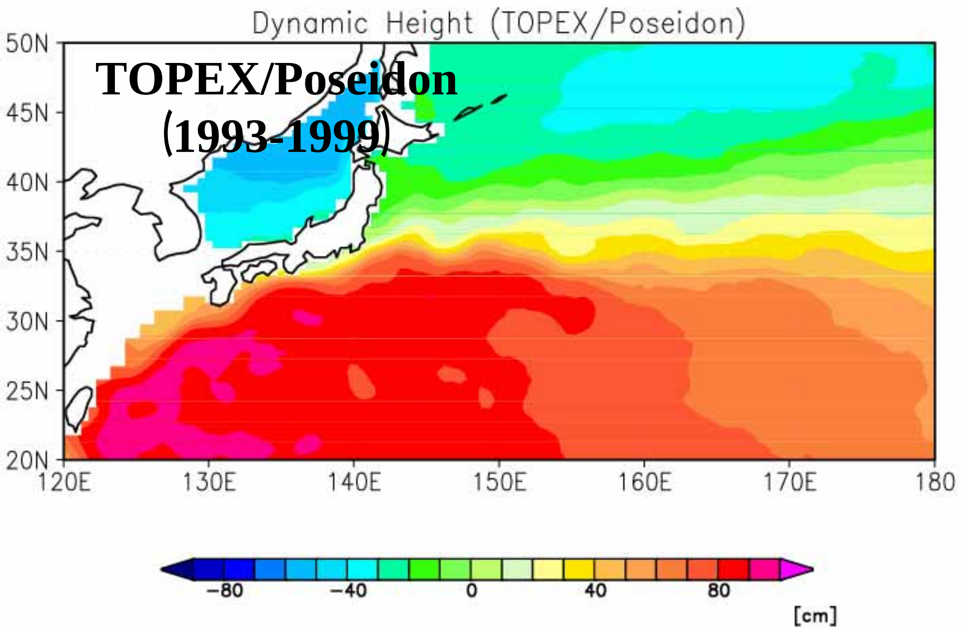

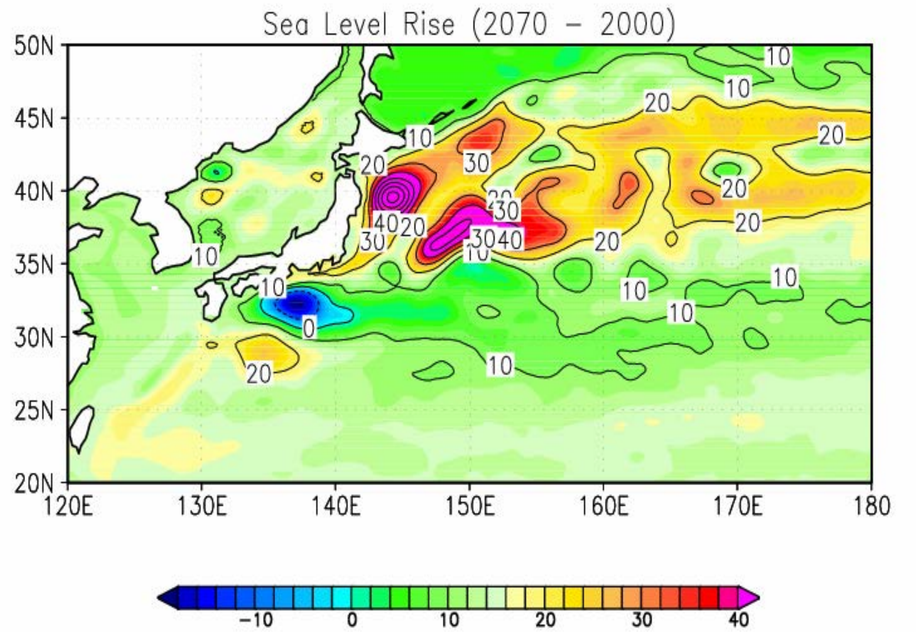

Climate Modeling at MRI

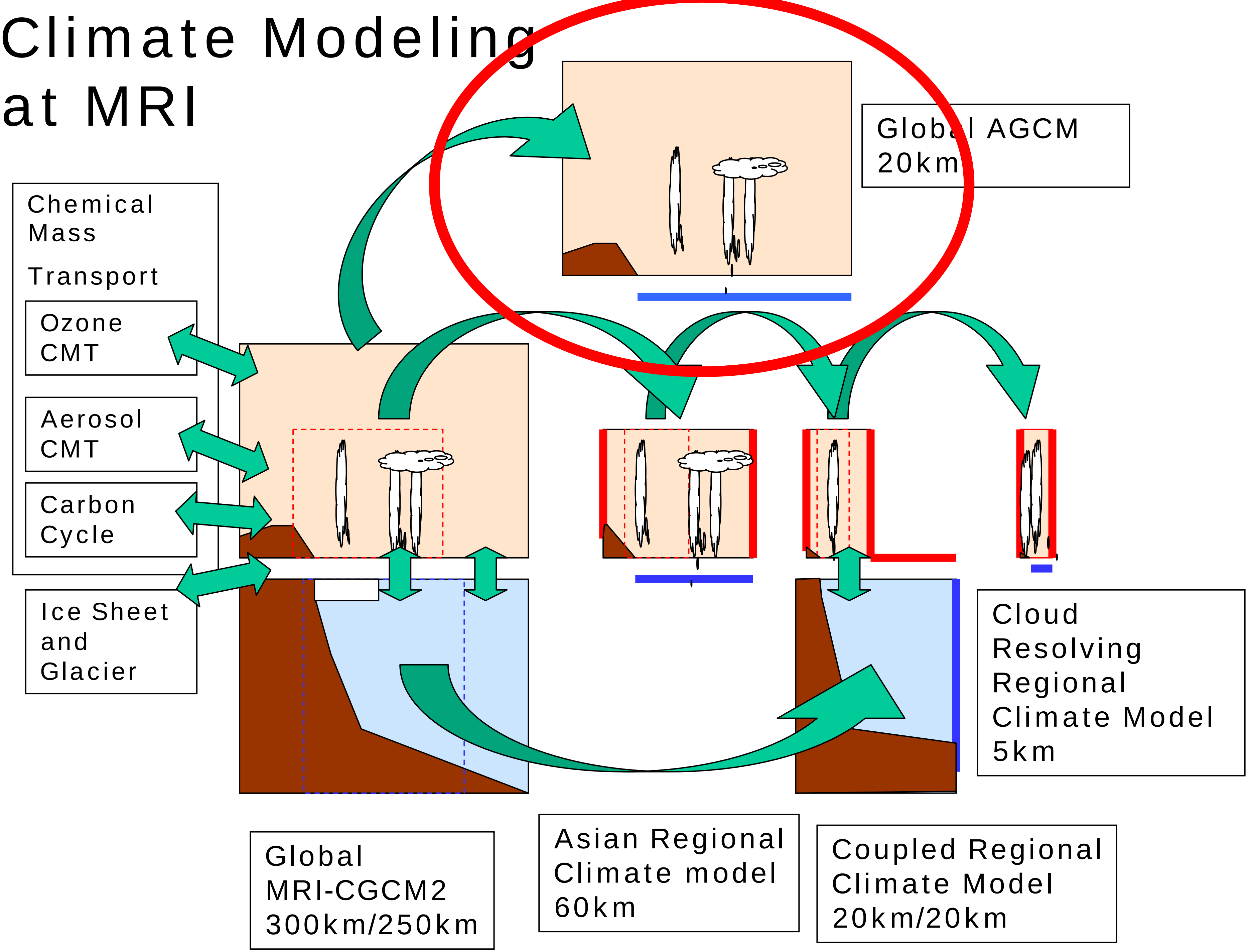

Earth Simulator

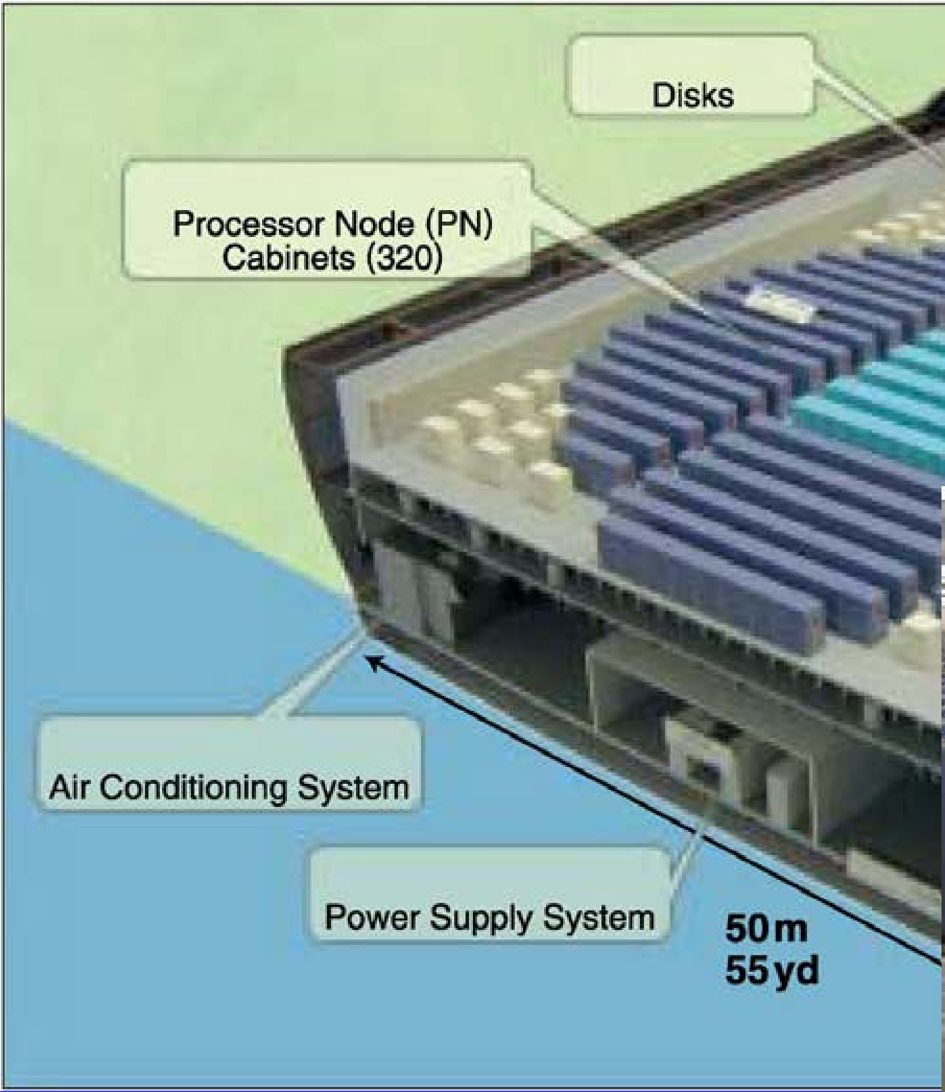

２０kmメッシュ全球気候モデルによる現在気候の再現

1時間降水量(mm)

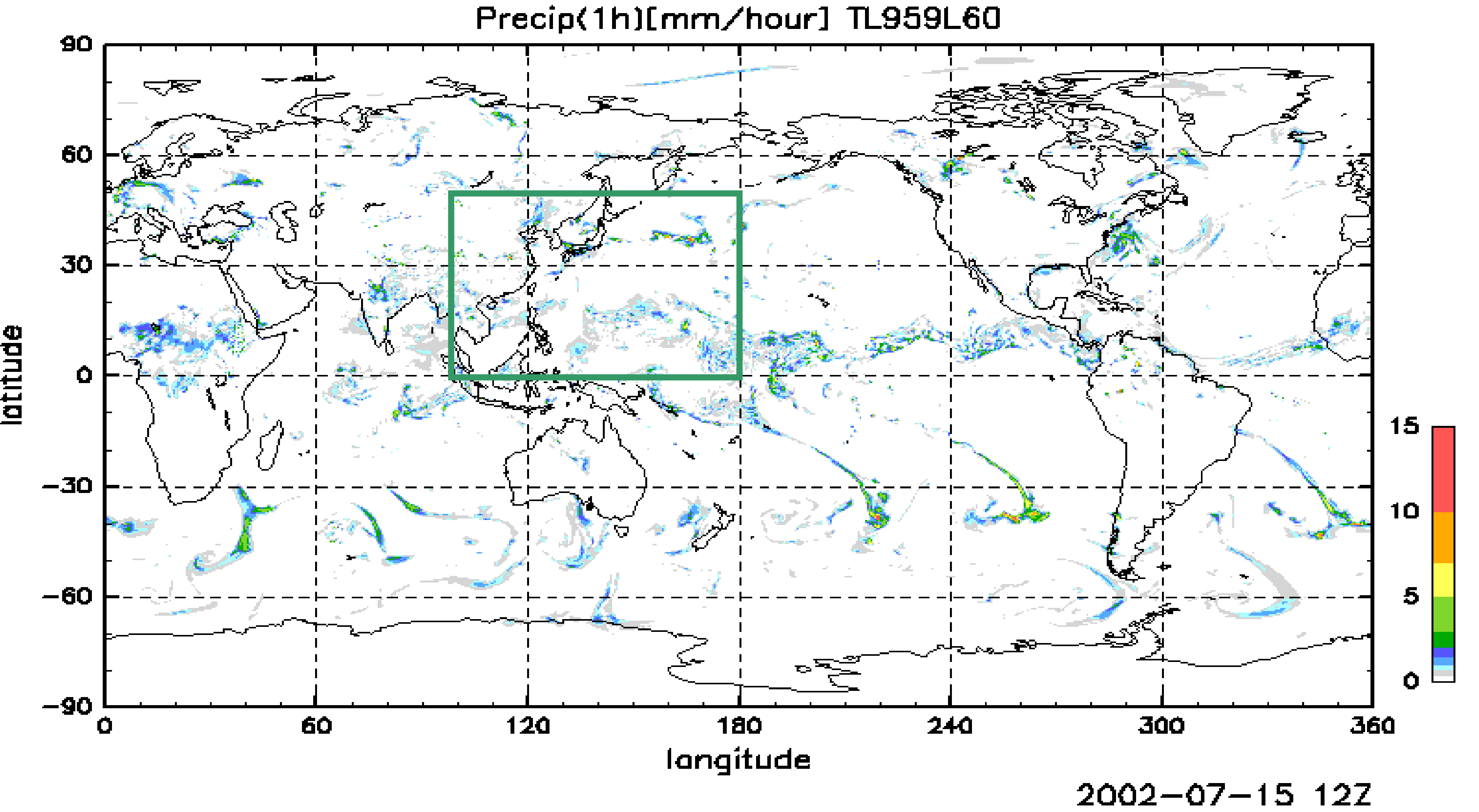

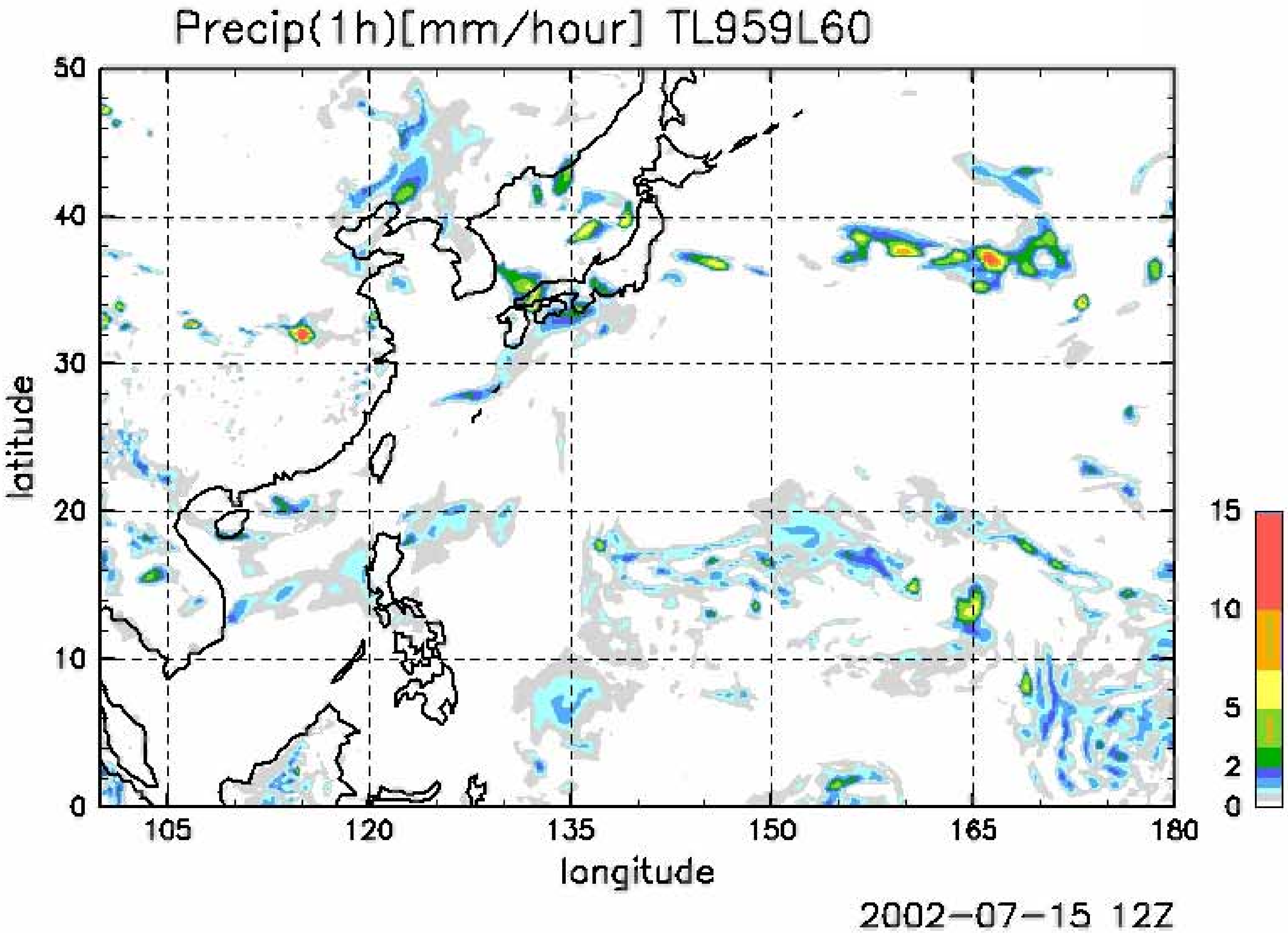

Precip(1h)[mm/hour] TL959L60
50
40
30
20
10
0
latitude
105
120
135
150
165
180
longitude
15
10
5
2
0
2002-07-15 12Z

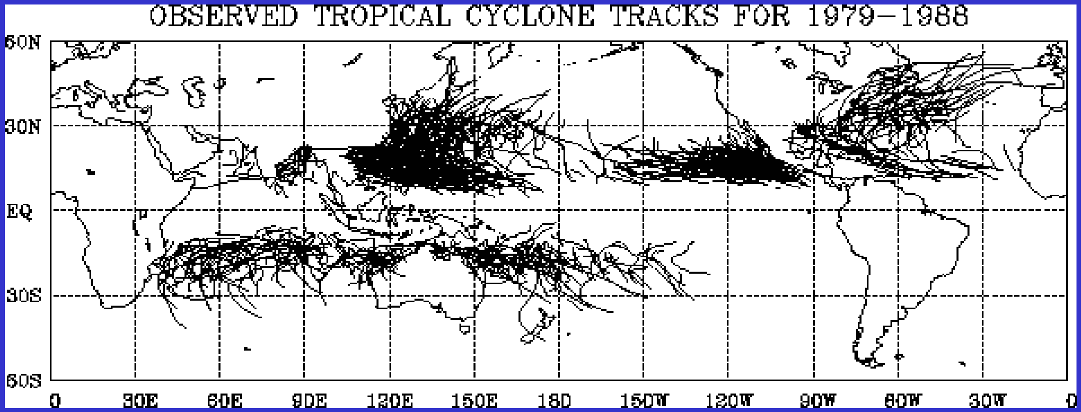

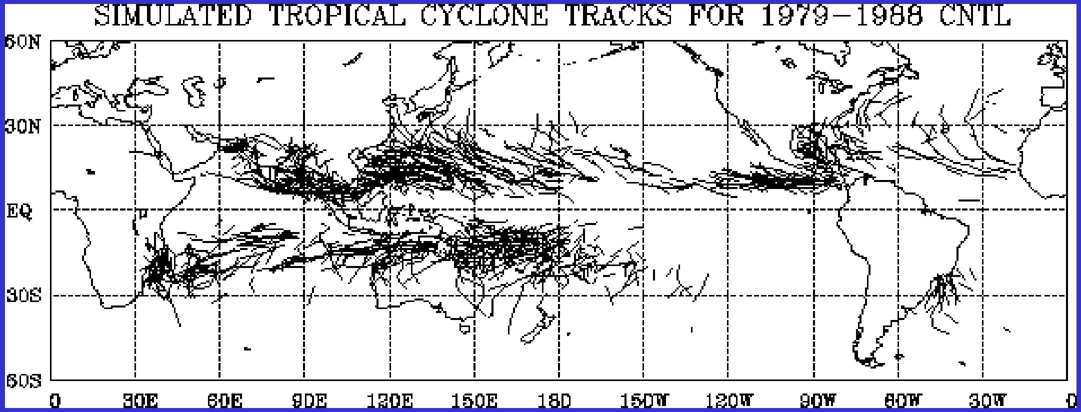

Simulations of Tropical Cyclones With AGCM of T106

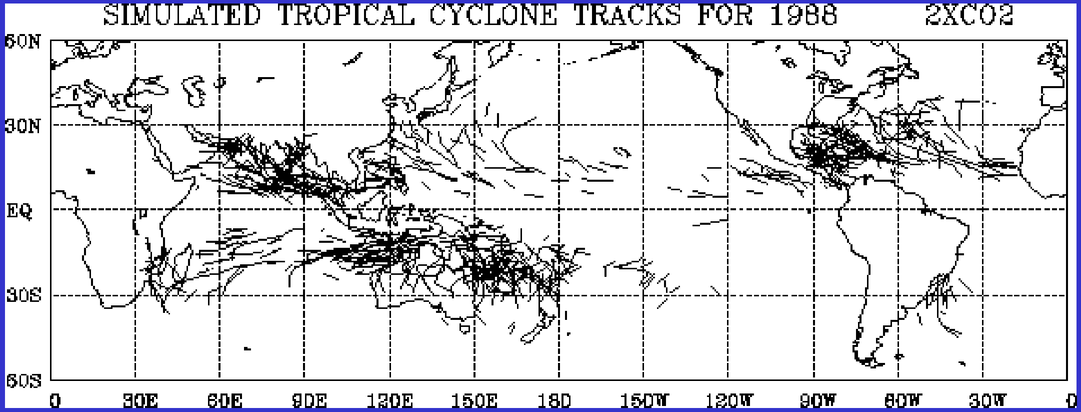

Sugi, Noda and Sato
(JMSJ, 2002)

More results are coming soon.

Acknowledgment

Computational resources are supplied by MRI, CGER/NIES and Earth Simulator.